JOURNAL OF BACTERIOLOGY, June 2010, p. 3144–3158 Vol. 192, No. 12
0021-9193/10/$12.00 doi:10.1128/JB.00031-10

RmpA Regulation of Capsular Polysaccharide Biosynthesis in *Klebsiella pneumoniae* CG43[▽]

H. Y. Cheng,[1] Y. S. Chen,[1] C. Y. Wu,[1] H. Y. Chang,[2] Y. C. Lai,[3] and H. L. Peng[1]*

Department of Biological Science and Technology, National Chiao-Tung University, Hsin Chu,[1] Institute of Molecular Medicine, National Tsing-Hua University, Hsin Chu,[2] and Department of Microbiology and Immunology, Chung-Shan Medical University, Tai Chung,[3] Taiwan, Republic of China

Received 13 January 2010/Accepted 30 March 2010

Sequence analysis of the large virulence plasmid pLVPK in *Klebsiella pneumoniae* CG43 revealed the presence of another mucoid factor encoding gene *rmpA* besides *rmpA2*. Promoter activity measurement indicated that the deletion of *rmpA* reduced K2 capsular polysaccharide (CPS) biosynthesis, resulting in decreased colony mucoidy and virulence in mice. Introduction of a multicopy plasmid carrying *rmpA* restored CPS production in the *rmpA* or *rmpA2* mutant but not in the *rcsB* mutant. Transformation of the *rmpA* deletion mutant with an *rcsB*-carrying plasmid also failed to enhance CPS production, suggesting that a cooperation of RmpA with RcsB is required for regulatory activity. This was further corroborated by the demonstration of *in vivo* interaction between RmpA and RcsB using two-hybrid analysis and coimmunoprecipitation analysis. A putative Fur binding box was only found at the 5′ noncoding region of *rmpA*. The promoter activity analysis indicated that the deletion of *fur* increased the *rmpA* promoter activity. Using electrophoretic mobility shift assay, we further demonstrated that Fur exerts its regulatory activity by binding directly to the promoter. As a result, the *fur* deletion mutant exhibited an increase in colony mucoidy, CPS production, and virulence in mice. In summary, our results suggested that RmpA activates CPS biosynthesis in *K. pneumoniae* CG43 via an RcsB-dependent manner. The expression of *rmpA* is regulated by the availability of iron and is negatively controlled by Fur.

Klebsiella pneumoniae, an important nosocomial pathogen, causes a wide range of infections, including pneumonia, bacteremia, urinary tract infection, and life-threatening septic shock (35). Clinically isolated *K. pneumoniae* strains usually produce a large amount of capsular polysaccharide (CPS), which confers not only a mucoid phenotype to the bacteria but also resistance to engulfment by professional phagocytes or to serum bactericidal factors (27, 37). CPS also plays a role in hindering fimbrial binding (39) and bactericidal effects resulting from antimicrobial peptides (5). The degree of mucoidy has been positively correlated with successful establishment of infection (31, 32). Most recently, the hypermucoviscosity of *K. pneumoniae* isolates has also been associated with the development of invasive syndrome (51). Among the identified serotypes, *K. pneumoniae* strains of K1 or K2 CPS are highly virulent in the mouse peritonitis model (30).

Klebsiella CPS resembles the *E. coli* group I CPS in primary structure and the mechanisms of biosynthesis (48). The chemical composition of *Klebsiella* K2 CPS, which contains uronic acid as the major component, has been determined as [→4-Glc-(1→3)-α-Glc-(1→4)-β-Man-(3←1)-α-GlcA)-(1→$_n$)] (45). Sequencing of the region responsible for K2 CPS biosynthesis in the *K. pneumoniae* Chedid strain revealed a total of 17 open reading frames organized into three transcriptional units (1). The two-component system (2CS) RcsBCD, which is the key regulatory system for *Escherichia coli* colonic acid synthesis, often serves as a model for group I CPS biosynthesis (19, 28). Upon receiving environmental stimuli, the transmembrane sensor kinase RcsC undergoes autophosphorylation, the signal is subsequently relayed to the inner membrane Hpt (for histidine-containing phosphotransfer) module RcsD and eventually to the cytoplasmic response regulator RcsB. The phosphorylated RcsB then interacts with RcsA, an auxiliary transcriptional regulator, and the heterodimer binds to the *cps* promoters, which in turn activates the biosynthesis of colanic acid capsule. RcsA is highly susceptible to degradation by the Lon protease; hence, *lon* mutation often leads to the accumulation of colanic acid (16). However, the introduction of multicopy *rcsB* has been shown to suppress the *rcsA*-negative phenotype (3).

K. pneumoniae CG43, with a 50% lethal dose (LD_{50}) of 10 CFU for laboratory mice, is a highly mucoid clinical isolate of K2 serotype (7). Its mucoid phenotype has been correlated with the presence of the large virulence plasmid pLVPK; curing of this plasmid has rendered an ~1,000-fold decrease in mouse virulence (12). We have also shown that *rmpA2* on pLVPK encodes a transcriptional activator for the *cps* expression by binding directly to the putative promoters, $P_{orf1\text{-}2}$ and $P_{orf3\text{-}15}$ (23). Interestingly, sequencing of the large virulence plasmid pLVPK revealed an *rmpA* gene 29 kb away from *rmpA2* (8). Excluding the extended 15 amino acids at the N terminus of RmpA2, the deduced RmpA sequence shares an overall 71.4% identity and a conserved C-terminal DNA binding motif with the RmpA2 protein.

An *rmpA* gene on the 180-kb virulence plasmid pKP100 of *K. pneumoniae* 52145 was reported 20 years ago (29). The encod-

* Corresponding author. Mailing address: Room 209, Chu-Ming Building, No.75, Bo-Ai St., Hsin Chu 30068, Taiwan, Republic of China. Phone: 886 3 5712121, ext. 56916. Fax: 886 3 5729288. E-mail: hlpeng@mail.nctu.edu.tw.

▽ Published ahead of print on 9 April 2010.

ing protein RmpA was subsequently demonstrated to be able to enhance colonic acid biosynthesis in *E. coli* HB101 (31). Later, the *rmpA2* gene, carrying an extended 5′ sequences of the *rmpA*, was isolated and shown to be able to activate K2 capsule production in the recombinant *E. coli* K-12 harboring *Klebsiella* K2 *cps* genes (45). We report here the characterization of RmpA in K2 CPS biosynthesis and comparative analysis of the expression of the two mucoid factor-encoding genes. We have demonstrated the interaction between RmpA and RcsB on the regulation of the CPS biosynthesis, and the involvement of Fur on the expression of *rmpA* has also been studied.

MATERIALS AND METHODS

Plasmids, bacterial strains, and growth conditions. The bacterial strains and plasmids used in the present study is listed in Table 1. *E. coli* and *K. pneumoniae* CG43 (7, 34) and its derivatives were propagated at 37°C in Luria-Bertani (LB) broth or M9 minimal medium as described previously (38). The antibiotics used include ampicillin (100 μg/ml), chloramphenicol (35 μg/ml), kanamycin (25 μg/ml), streptomycin (500 μg/ml), and tetracycline (12.5 μg/ml). The primers used in the present study are listed in Table 2.

RT-PCR and Southern blotting analysis. Total RNA was extracted from log-phase *K. pneumoniae* cells (optical density at 600 nm [OD_{600}] of 0.6 to 0.8) with the TriReagent (Molecular Research Center, Cincinnati, OH). RQ1 RNase-free DNase (Promega, Madison, WI) was used to eliminate contaminating DNA. Reverse transcription (RT) was carried out with 1 to 2 μg of DNA-free RNA samples using Moloney murine leukemia virus (MMLV) reverse transcriptase (Promega, Madison, WI). The resulting cDNA was then used as the template for PCR amplification using *Taq* polymerase with the primers rmpA06 and rmpA07 (Table 2). The PCR products were resolved on agarose gels by electrophoresis, and the DNA fragments were transferred onto a nitrocellulose membrane and fixed by using a UV cross-linker (SpectroLinker XL-1000). The membrane was then subjected to hybridization with the fluorescein-labeled *rmpA* gene probe, and the signal was detected according to the manufacturer's instruction (CDP-Star DNA labeling and detection kit; Roche Molecular Biochemicals, Indianapolis, IN).

Construction of the gene deletion mutants and complementation plasmids. Specific gene deletion was introduced into *K. pneumoniae* CG43 by using an allelic-exchange strategy as previously described (23). In brief, two ~1,000-bp DNA fragments flanking both sides of the deleted region were cloned into pKAS46 (40), a suicide vector containing *rpsL*, which allows positive selection with streptomycin for vector loss. The resulting plasmids were mobilized from *E. coli* S17-1λ*pir* (25) to *K. pneumoniae* CG43S3 or CG43S3Δ*lacZ*, by conjugation, respectively. The transconjugants, with the plasmid integrated into the chromosome via homologous recombination, were selected with ampicillin and kanamycin on M9 agar plates. Several of the colonies were grown overnight in LB broth at 37°C and then spread onto an LB agar plate containing 500 μg of streptomycin/ml. Streptomycin-resistant and kanamycin-sensitive colonies were selected, and the deletion was verified by PCR and Southern analysis using a gene-specific probe. The resulting mutant strains are listed in Table 1.

To obtain the complementation plasmids, DNA fragments containing the *rmpA*, *rmpA2*, *rcsB*, and *fur* loci were PCR amplified by using the primer pairs Yu05/Yu06, rmpA2p06/rmpA2p07, rcsBc01/rcsBc02, and CY007/CY008 (Table 2), and the PCR products were cloned into pRK415 (20) to generate pRK415-RmpA, pRK415-RmpA2, pRK415-RcsB, and pRK415-Fur, respectively. Plasmid pRK415-RmpAN carries a truncated form of RmpA (RmpAN) of residues 1 to 84 (Table 1).

Extraction and quantification of CPS. The bacterial CPS was extracted by using a method described earlier (9). Briefly, 500 μl of overnight grown bacteria was mixed with 100 μl of 1% Zwittergent 3-14 (Sigma-Aldrich, Milwaukee, WI) in 100 mM citric acid (pH 2.0) and then incubated at 50°C for 20 min. After centrifugation, 250 μl of the supernatant was transferred to a new tube, and the CPS was precipitated with 1 ml of absolute ethanol. The pellet was dried and dissolved in 200 μl of distilled water, and then 1,200 μl of 12.5 mM borax in H_2SO_4 was added. The mixture was vigorously mixed, boiled for 5 min, and cooled, and then 20 μl of 0.15% 3-hydroxydiphenol (Sigma-Aldrich, Milwaukee, WI) was added. The absorbance at 520 nm was measured, and the uronic acid content was determined from a standard curve of glucuronic acid and expressed as micrograms per 10^9 or 10^{10} CFU.

Mouse lethality assay. The virulence in mice was determined as previously described (23). Female BALB/c mice (4 to 5 weeks old) were obtained from the National Laboratory Animal Center and acclimatized in an animal house for 7 days. The tested bacterial strains were cultured in LB medium at 37°C overnight. Four mice of a group were injected intraperitoneally with 0.2 ml of bacterial suspension in saline in 10-fold graded doses. Based on the number of survivors after 14 days, the LD_{50} values were calculated by using the Reed and Muench method (36) and are expressed as CFU.

Bacterial survival in serum. Bacterial survival in serum was determined with minor modifications (23). First, 100 μl of bacterial suspension in saline was mixed with 100 μl of pooled serum from healthy volunteers, and the mixture was incubated at 37°C for 30 min. The number of viable bacteria was then determined by plate counting. The survival rate was expressed as the number of viable bacteria treated with human serum compared to the number of those incubated with phosphate-buffered saline. The assay was performed twice, each with triplicate samples. The data from one of the representative experiments are shown and expressed as the mean and standard deviation from the three samples. A 0% survival of *K. pneumoniae* CG43S3Δ*galU* (23) served as a negative control.

Measurement of promoter activity. The promoter reporter plasmids were individually mobilized into *K. pneumoniae* strains by conjugation from *E. coli* S17-1λ*pir*. The β-galactosidase activity was measured as described previously (25). In brief, the bacteria was grown to the log phase in LB medium (OD_{600} of 0.7) or M9-glucose medium (OD_{600} of 0.5), and 100 μl of the culture was mixed with 900 μl of Z buffer (60 mM Na_2HPO_4, 40 mM NaH_2PO_4, 10 mM KCl, 1 mM $MgSO_4$, 50 mM β-mercaptoethanol), 17 μl of 0.1% sodium dodecyl sulfate (SDS), and 35 μl of chloroform, followed by vigorous shaking. After incubation at 30°C for 10 min, 200 μl of a 4-mg/ml concentration of o-nitrophenyl-β-D-galactopyranoside (ONPG; Sigma-Aldrich, Milwaukee, WI) was added to the mixture to initiate the reaction. When yellow coloration was apparent, the reaction was stopped by adding 500 μl of 1 M Na_2CO_3 to the mixture, and the absorbance at OD_{420} was recorded; the activity was expressed as Miller units (29). Each sample was assayed in triplicate, and at least three independent experiments were carried out. The data shown were calculated from one representative experiment and are shown as the means and standard deviation from triplicate samples.

Construction of the plasmid for K2 *cps* $P_{orf1\text{-}2}$::*lacZ* chromosomal fusion. The $P_{orf1\text{-}2}$::*lacZ* cassette from pOrf12 (25) was subcloned into pKAS46; the resulting plasmid was mobilized into *K. pneumoniae* CG43S3Δ*lacZ*, CG43S3Δ*rcsB*Δ*lacZ*, or CG43S3Δ*rmpA*Δ*lacZ* via conjugation from *E. coli* S17-1λ*pir*. The transconjugants were screened by counterselection on M9 agar plate supplemented with kanamycin and X-Gal (5-bromo-4-chloro-3-indolyl-β-D-galactopyranoside). After overnight incubation at 37°C, blue colonies, in which the reporter cassette was integrated into the chromosomal *cps* region via the $P_{orf1\text{-}2}$ by homologous recombination, were isolated. The integration of the reporter cassette in the resulting strains was further confirmed by PCR with the primers CH009/CH010 (Table 2).

Bacterial two-hybrid analysis. The DNA fragments encoding full-length RcsA, RmpA, RmpAN, or RmpA2 were PCR amplified with the primer sets rcsAe04/rcsAe07, rmpAe04/rmpAe05, or rmpA2p08/rmpA2p14 (Table 2) and cloned to the 3′ end of the gene encoding the λ-cI repressor protein domain on the NotI/XhoI site in pTRG to generate pTRG-RcsA, pTRG-RmpA, pTRG-RmpAN, or pTRG-RmpA2, respectively. The DNA fragments encoding the full-length RcsB were PCR amplified with primers rcsBe02/rcsBe04 (Table 2) and cloned to the 3′ end of the gene encoding the α subunit of RNA polymerase (RNAPα) domain on the NotI/XhoI site in pBT to generate pBT-RcsB. The resulting plasmids were confirmed by DNA sequencing. The pBT and pTRG derived plasmids were cotransformed into *E. coli* XL1-Blue MRF′ Kan cells, and the transformants were selected on LB agar plates containing 12.5 μg of tetracycline/ml, 25 μg of chloramphenicol/ml, and 50 μg of kanamycin/ml, essentially as described previously (18, 22). To investigate the protein-protein interaction *in vivo*, the bacteria were grown in LB medium at 30°C until the OD_{600} reached 0.4 and then diluted serially (10^{-2}, 10^{-3}, 10^{-4}, and 10^{-5}). Two microliters of the bacterial culture was spotted onto the indicator plate (LB agar plate supplemented with 350 μg of carbenicillin/ml, 25 μg of chloramphenicol/ml, 50 μg of kanamycin/ml, 12.5 μg of tetracycline/ml, 50 μg of X-Gal/ml, and 20 μM IPTG (isopropyl-β-D-thiogalactopyranoside). After the plates were incubated at 30°C for 48 h, the growth of the bacterial cells was observed.

For the measurement of β-galactosidase activities, *E. coli* strains carrying different combinations of the recombinant plasmids were grown for 48 h at 30°C. After washing with LB, the bacteria were grown at 30°C to an OD_{600} of 0.5. IPTG was then added to a final concentration of 20 μM, and the cultures were incubated at 30°C for another 16 h. Finally, the β-galactosidase activity was determined and calculated as described above.

Cloning, expression, and purification of the recombinant proteins. The coding region of *rcsB* or *fur* was PCR amplified with the primer sets rcsBe01/rcsBe02 or

TABLE 1. Bacterial strains and plasmids used in this study

Strain or plasmid	Genotype or description[a]	Reference or source
Strains		
K. pneumoniae		
CG43	Clinical isolate	34
CG43S3	CG43 Sm^r	23
CG43S3Δ*rmpA*	CG43S3 Δ*rmpA* Sm^r	This study
CG43S3Δ*rmpA2* (R2035)	CG43S3 Δ*rmpA2* Sm^r	23
CG43S3Δ*rmpA*Δ*rmpA2*	CG43S3 Δ*rmpA* Δ*rmpA2* Sm^r	This study
CG43S3Δ*rcsB* (B2202)	CG43S3 Δ*rcsB* Sm^r	23
CG43S3Δ*fur*	CG43S3 Δ*fur* Sm^r	This study
CG43S3Δ*lacZ* (Z01)	CG43S3 Δ*lacZ* Sm^r	25
CG43S3Δ*rmpA*Δ*lacZ*	CG43S3 Δ*lacZ* Δ*rmpA* Sm^r	This study
CG43S3Δ*rmpA2*Δ*lacZ*	CG43S3 Δ*lacZ* Δ*rmpA2* Sm^r	This study
CG43S3Δ*fur*Δ*lacZ*	CG43S3 Δ*lacZ* Δ*fur* Sm^r	This study
CG43S3Δ*rcsB*Δ*lacZ* (RcsBZ01)	CG43S3 Δ*lacZ* Δ*rcsB* Sm^r	25
CG43S3Δ*galU* (U9451)	CG43S3 Δ*galU* Sm^r	Laboratory stock
E. coli		
S17-1λ*pir*	*hsdR recA pro* RP4-2 (Tc::Mu Km::Tn*7*) (λ*pir*)	40
BL21(DE3)	F′ *ompT hsdS*$_B$ (r_B^- m_B^-) *gal dcm trxB15*::*kan* (DE3)	Novagen
BL21(DE3)/pLysS	F′ *ompT hsdS*$_B$ (r_B^- m_B^-) *gal dcm trxB15*::*kan* (DE3)/pLysS	Novagen
XL-1 Blue MRF′ Kan	Δ*mcrA 183*Δ[(*mcrCB-hsdSMR-mrr*)*173 endA1 supE44 thi-1 recA1 gyrA96 relA1 lac* (F′ *proAB lacI*^{q}*Z*ΔM15 Tn*5*(Km^r))]	Novagen
Plasmids		
pBT	Cm^r; bait plasmid, *p15A* origin of replication, *lac-UV5* promoter, λ-cI open reading frame	Stratagene
pTRG	Tc^r; target plasmid, ColE1 origin of replication, *lac-UV5* promoter, *RNAP*α open reading frame	Stratagene
pET30b-c	His-tagged protein expression vector; Km^r	Novagen
pBT-LGF2	Cm^r; control plasmid containing a fragment encoding the yeast transcriptional activator Gal4 fused with λ-cI	Stratagene
pTRG-GAL11^P	Tc^r; control plasmid containing a fragment encoding a mutant form of Gal11 protein, called Gal11P, fused with RNAPα	Stratagene
pGEX-5X-1	Ap^r; GST-tagged protein expression vector	GH Hleathcare
yT&A	Ap^r; T/A-type PCR cloning vector	Yeastern
pKAS46	Ap^r Km^r; suicide vector, *rpsL*	40
pRK415	Tc^r; shuttle vector, *mob*$^+$	20
pACYC184	Cm^r Tc^r; plasmid with *p15A* origin of replication	6
pYC084	Tc^r; 2.1-kb HindIII/BamHI fragment containing the entire *rmpA2* locus cloned into pRK415	23
placZ15	Cm^r; promoter selection vector, *lacZ*$^+$	25
pOrf12	Cm^r; 500-bp fragment containing the region upstream of *Klebsiella* K2 *cps orf1-orf2* cloned into placZ15	25
pOrf315	Cm^r; 900-bp fragment containing the region upstream of *Klebsiella* K2 *cps orf3-orf15* cloned into placZ15	25
pOrf1617	Cm^r; 300-bp fragment containing the region upstream of *Klebsiella* K2 *cps orf16-orf17* cloned into placZ15	25
pRK415-RcsB	Tc^r; 1.2-kb fragment containing the entire *rcsB* locus cloned into pRK415	This study
pRK415-RmpA	Tc^r; 1.1-kb fragment containing the entire *rmpA* locus cloned into pRK415	This study
pRK415-RmpAN	Tc^r; 1.1-kb fragment containing the *rmpA* locus encoding a truncated form of RmpA (residues 1 to 84) cloned into pRK415	This study
pRK415-RmpA2	Tc^r; 1.2-kb fragment containing the entire *rmpA2* locus cloned into pRK415	This study
pHY083	Ap^r Km^r; the P$_{orf1-2}$::*lacZ* reporter cassette cloned into pKAS46	This study
pBT-RcsB	Cm^r; 648-bp fragment encoding full-length RcsB cloned into pBT	This study
pTRG-RcsA	Tc^r; 621-bp fragment encoding full-length RcsA cloned into pTRG	This study
pTRG-RmpAN	Tc^r; 252-bp fragment encoding residues 1-84 of RmpA cloned into pTRG	This study
pTRG-RmpA2	Tc^r; 636-bp fragment encoding full-length RmpA2 cloned into pTRG	This study
pGEX-RcsA	Ap^r; 621-bp fragment encoding full-length RcsA cloned into pGEX-5X-1	This study
pGEX-RmpA	Ap^r; 585-bp fragment encoding full-length RmpA cloned into pGEX-5X-1	This study
pGEX-RmpAN	Ap^r; 252-bp fragment encoding residues 1 to 84 of RmpA cloned into pGEX-5X-1	This study
pGEX-RmpA2	Ap^r; 636-bp fragment encoding full-length RmpA2 cloned into pGEX-5X-1	This study
pET30b-RcsB	Km^r, 648-bp fragment encoding full-length RcsB cloned into pET30b	This study
pACYC184-RcsB	Tc^r; 1.1-kb EcoRI fragment containing full-length RcsB-His_6 and the upstream T7 promoter region from pET30b-RcsB cloned into pACYC184	This study
placZ15-PrmpA	Cm^r; 500-bp fragment containing the region upstream of *rmpA* cloned into placZ15	This study
placZ15-PrmpA2	Cm^r; 500-bp fragment containing the region upstream of *rmpA2* cloned into placZ15	This study
placZ15-PiucA	Cm^r; 700-bp fragment containing the region upstream of *iucABCD* cloned into placZ15	This study
placZ15-PiroB	Cm^r; 450-bp fragment containing the region upstream of *iroBCD* cloned into placZ15	This study
pET30c-Fur	Km^r; 450-bp fragment encoding full-length Fur cloned into pET30c	This study
pRK415-Fur	Tc^r; 0.8-kb fragment containing the entire *fur* locus cloned into pRK415	This study

[a] Cm^r, chloramphenicol resistance; Tc^r, tetracycline resistance; Ap^r, ampicillin resistance; Sm^r, streptomycin resistance; Km^r, kanamycin resistance.

TABLE 2. Oligonucleotide primers used in this study

Primer	Sequence (5′–′3)[a]	Enzyme cleaved	Complementary position
CH009	AGCGTGACGAGACCTGCCCA	None	−802 relative to the K2 *cps orf1* start codon
CH010	GGCTGCGGGCGTAAGAGAAC	None	+217 relative to the *lacZ* start codon
CY007	TCTAGAGGCAGGTTGGCTCTTCAGTC	XbaI	+489 relative to the *fur* start codon
CY008	GGATCCATGAAGACAGCCAGCCGGA	BamHI	−389 relative to the *fur* start codon
CY0010	GGATCCGATTCCGCATGACTGACAAC	BamHI	−8 relative to the *fur* start codon
CY0011	AAGCTTGGCAGGTTGGCTCTTCAGTC	HindIII	+489 relative to the *fur* start codon
pET30f2	TTGAATTCTAGGTTGAGGCCGTTGAGCA	EcoRI	+673 to +692 region on pET30a
pET30r2	CAAGAATTCAAACCCCTCAAGACCCGT	EcoRI	+31 to +47 region on pET30a
Pirop01	GGATCCGATTTCAGTACGGCATGGAC	BamHI	−379 relative to the *iroB* start codon
Pirop02	AGATCTACGGGAAACGCCTGTGCCA	BglII	+77 relative to the *iroB* start codon
Piucp01	GGATCCAGAGGGTGATTTGCCAGCAT	BamHI	−611 relative to the *iucA* start codon
Piucp02	AGATCTGGAAGCACTGAGCAGCCACA	BglII	+109 relative to the *iucA* start codon
rcsAe04	GTTTGTTTCACTCGAGGCGCATATTTACC	XhoI	+631 relative to the *rcsA* start codon
rcsAe07	CTAGCGGCCGCGATGTCAACGATGATTATGGATT	NotI	+1 relative to the *rcsA* start codon
rcsAe08	CTAGGATCCCCATGTCAACGATGATTATGGATT	BamHI	+1 relative to the *rcsA* start codon
rcsBc01	CCCGGATCCAACTGCGGGTCAACTTT	BamHI	−398 relative to the *rcsB* start codon
rcsBc02	CCCGGATCCTTGTCTGTCCAAGCCGGTCA	BamHI	+781 relative to the *rcsB* start codon
rcsBe01	GGCCGCCTTATACCATATGAACACTA	NdeI	+1 relative to the *rcsB* start codon
rcsBe02	CCCTCGAGCTCTTTGTCCGTCGCGCTC	XhoI	+648 relative to the *rcsB* start codon
rcsBe04	CTCGCGGCCGCGATGAACACTATGAACGTAATTAT	NotI	−1 relative to the *rcsB* start codon
rmpA06	TTACCTAAATACTTGGCATGAGC	None	+592 relative to the *rmpA* start codon
rmpA07	CAAGGATCCAAAGCATAGTGTT	BamHI	−17 relative to the *rmpA* start codon
rmpAc01	CCCGGATCCAGAAACAGACAGTATTACTAAGCGAA	BamHI	−384 relative to the *rmpA* start codon
rmpAe04	CCCTTTTTTACCTCGAGAATACTTGGCATGA	XhoI	+585 relative to the *rmpA* start codon
rmpAe05	CTTGCGGCCGCGGTGTTGACTGATGATTATTTTTTTTA	NotI	+1 relative to the *rmpA* start codon
rmpAe07	CTTGGATCCCCGTGTTGACTGATGATTATTTTTTTA	BamHI	−2 relative to the *rmpA* start codon
rmpAp04	CCCAGATCTCAGTCAACACGGTGCTTTAC	BglII	+10 relative to the *rmpA* start codon
rmpAp05	CCCGGATCCAACTCGCCCCTCCCCACAC	BamHI	−308 relative to the *rmpA* start codon
rmpAp11	CCAGGATCCTACCGTGATTGATTGAATTTTTA	BamHI	−184 relative to the *rmpA* start codon
rmpAp12	GTCGGATCCATCGCCAAATAACTC	BamHI	−479 relative to the *rmpA* start codon
rmpAp13	TCAATTAATTGCAAACACGC	None	−226 relative to the *rmpA* start codon
rmpAt01	ACAGAGGTAGTCCAGTTAACA	None	+61 relative to the *rmpA* start codon
rmpA2p06	CCCGGATCCCACTTAGTCCTGTGTC	BamHI	−391 relative to the *rmpA2* start codon
rmpA2p07	GATGGATCCCTAGGTATTTGATGTGCAC	BamHI	+639 relative to the *rmpA2* start codon
rmpA2p08	GATCTCGAGGGTATTTGATGTGCAC	XhoI	+639 relative to the *rmpA2* start codon
rmpA2p14	CCCGCGGCCGCGATGGAAAAATATATTTACTT	NotI	−1 relative to the *rmpA2* start codon
rmpA2p17	CCCGGATCCCCATGGAAAAATATATTTACTT	BamHI	+1 relative to the *rmpA2* start codon
Yu05	CCTTCACATCCCCTCCCCTT	None	+614 relative to the *rmpA* start codon
Yu06	GTCGGATCCATCGCCAAATAA	None	−479 relative to the *rmpA* start codon
GSPrmpA01	TTAGGATAAAACCGCCCCCCCCCCGAAAC	None	+254 relative to the *rmpA* start codon
GSPrmpA02	CATTTTGTACCCTCCCCATTTCCCTGA	None	+180 relative to the *rmpA* start codon
RTrmpA01	TGATGGATCAAAGTTACTGT	None	−70 relative to the *rmpA* start codon
RTrmpA02	TCCCTGAATAAAAAATCCTGCTGTC	None	+160 relative to the *rmpA* start codon
23SF	AGCGACTAAGCGTACACGGTGG	None	+4 relative to the *rrnB* start codon
23SR	GATGTTTCAGTTCCCCCGGTTC	None	+200 relative to the *rrnB* start codon

[a] The nucleotide sequence recognized by each restriction enzyme is indicated by underlining.

CY0010/CY0011 (Table 2) and cloned into the NdeI/XhoI site in pET30b (Novagen, Madison, WI) or the BamHI/HindIII site in pET30c, respectively. This generates pET30b-RcsB with a carboxyl-terminus His tag (RcsB-His_6) or pET30c-Fur with an amino-terminus His tag (His_6-Fur). The resulting plasmid pET30b-RcsB or pET30c-Fur was then transformed into *E. coli* BL21(DE3)/pLysS (Invitrogen), and overproduction of the recombinant protein was induced by the addition of 0.5 mM IPTG for 4 h at 37°C. The recombinant proteins were then purified from the soluble fraction of the total cell lysate by affinity chromatography using His-Bind resin (Novagen). Finally, the purified proteins were dialyzed against 1× TBS (Tris-buffered saline; pH 7.4) containing 10% glycerol at 4°C overnight, followed by condensation with PEG 20000, and the purity was determined by SDS-PAGE.

Preparation of RcsB-His_6 antiserum. The RcsB-His_6 antiserum was prepared by immunizing 5-week-old female BALB/c mice purchased from the animal center of National Taiwan University intraperitoneally with 10 mg of purified RcsB-His_6. Ten days later, the mice were immunized again with 10 mg of the same protein, and the antiserum was obtained via intracardiac puncture.

Construction of GST fusion plasmids and coimmunoprecipitation (IP). To obtain the glutathione *S*-transferase (GST) fusion plasmids, the DNA fragments encoding full-length RcsA, RmpA, RmpAN, or RmpA2 were PCR amplified with the primer sets rcsAe04/rcsAe08, rmpAe04/rmpAe07, or rmpA2p08/rmpA2p17 (Table 2) and cloned into the BamHI/XhoI site in pGEX-5X-1 (GE Healthcare) to generate pGEX-RcsA, pGEX-RmpA, pGEX-RmpAN, or pGEX-RmpA2 (Table 1), respectively. To construct an RcsB-His_6 expression plasmid compatible with pGEX-5X-1, the DNA fragment containing the entire RcsB-His_6 coding sequence and the upstream T7 promoter region was PCR amplified with the primers pET30f2 and pET30r2 (Table 2) and cloned into an EcoRI site on pACYC184 to generate pACYC184-RcsB. To perform coimmunoprecipitation, different combinations of the expression plasmids were cotransformed into *E. coli* BL21(DE3). The transformants were grown overnight in LB medium at 37°C and grown in refreshed LB medium at 37°C to an OD_{600} of 0.5. IPTG was then added to a final concentration of 1 mM, and the cultures were incubated at 25°C for another 16 h. The cells were recovered by centrifugation, resuspended in 500 μl of IP buffer (1× TBS [pH 7.4], 0.1% [wt/vol] bovine serum albumin [BSA], 1× protease inhibitor cocktail set VII [Calbiochem, La Jolla, CA]), and disrupted by sonication on ice. After centrifugation at 4°C, the supernatant was collected as preimmunoprecipitation (Pre-IP) samples. Ten micrograms of each Pre-IP sample was subjected to SDS-PAGE and immunoblotted with anti-GST or anti-His_6 monoclonal antibody to ensure the expression of the recombinant proteins. For IP analysis, 500 μg of total protein for each sample

was incubated with ~50 μl of glutathione-Sepharose 4 Fast Flow (GE Healthcare) in a final volume of 500 μl. After incubation at 4°C for 3 h with end-over-end mixing, the beads were collected by centrifugation, washed three times with 500 μl of ice-cold IP buffer containing 1% (vol/vol) Triton X-100, and washed once with 500 μl of ice-cold IP buffer containing 1% Triton X-100 and 1 M NaCl. Finally, the beads were washed with 500 μl of ice-cold IP buffer containing 1% Triton X-100 to remove the residual salts and mixed with 50 μl of 1× SDS-PAGE sample buffer. The samples were boiled at 95°C for 10 min and subjected to SDS-PAGE and immunoblot analysis with anti-His_6 monoclonal antibody or anti-RcsB-His_6 polyclonal antiserum. The presence of proteins was visualized by an alkaline phosphatase-mediated chromogenic substrate reaction.

DNA electrophoretic mobility shift assay (EMSA). The DNA fragments P1 to P6 were PCR amplified with the primer sets Piucp01/Piucp02, Pirop01/Pirop02, rmpAp04/rmpAp12, rmpAp04/rmpAc01, rmpAp04/rmpAp13, and rmpAp04/rmpAp11 (Table 2), respectively, and end labeled with [γ-^{32}P]ATP using T4 polynucleotide kinase as described previously (23). The purified His_6-Fur protein was mixed with labeled probes (~0.1 ng) in a 50-μl reaction mixture containing 50 mM Tris-HCl (pH 7.5), 100 mM NaCl, 0.1 mM EDTA, 10 mM dithiothreitol, and 0.5 μg of BSA/μl. The mixture was incubated at room temperature for 30 min, mixed with a 0.1× volume of DNA loading dye, loaded onto a 5% nondenaturing polyacrylamide gel containing 5% glycerol, and then run in a 0.5× TB buffer (45 mM Tris-HCl [pH 8.0], 45 mM boric acid) containing 100 μM $MnCl_2$. After electrophoresis at a constant current of 20 mA at 4°C for 2 h, the results were detected by autoradiography.

Identification of *rmpA* transcriptional start site. For the determination of *rmpA* 5′-mRNA ends, a 5′-RACE (5′ rapid amplification of cDNA ends) PCR was performed by using a 5′-RACE kit (Clontech, Mountain View, CA) according to the manufacturer's instruction. In brief, total RNA was isolated from log-phase *K. pneumoniae* CG43S3 and Δ*fur* mutant grown in LB medium by using a High-Pure RNA isolation kit (Roche, Mannheim, Germany). One microgram of total RNA was treated with RNase-free DNase I (Roche) and recovered by phenol-chloroform extraction. For the first-strand cDNA synthesis, a 3.75-μl reaction mixture containing 1 μg of DNase-treated RNA and random primer mix (N-15) was incubated at 72°C for 3 min and then reduced to room temperature for 5 min before the addition of 5× first-strand buffer, deionized water, dithiothreitol, deoxynucleoside triphosphate mix, RNase inhibitor, SMARTer II A oligonucleotide, and SMARTScribe reverse transcriptase to a final volume of 10 μl. The reaction mixture was incubated at room temperature for 10 min, 42°C for 90 min, and 72°C for 10 min to terminate the reaction; diluted with 20 μl of Tricine-EDTA buffer; and then stored at −20°C. For the primary PCR, a 50-μl reaction mixture containing diluted cDNA templates, gene-specific primer, universal primer mix, deoxynucleoside triphosphate mix, PCR buffer, deionized water, and DNA polymerase was prepared. The reaction mixture without reverse transcriptase served as a negative control template. The PCR program consisted of 5 cycles of 30 s at 94°C and 3 min at 72°C; 5 cycles of 30 s at 94°C, 30 s at 70°C, and 3 min at 72°C; and 25 cycles of 30 s at 94°C, 30 s at 68°C, and 3 min at 72°C. For the nested PCR, the reaction mixture was essentially the same as the primary PCR mixture except that 100-fold-diluted primary PCR product as the template, gene-specific primer, and nested universal primer were used. The PCR program consisted of 25 cycles of 30 s at 94°C, 30 s at 60°C, and 3 min at 72°C. The PCR products were resolved on an agarose gel by electrophoresis, and the DNA fragments were recovered and cloned into the PCR cloning vector yT&A (Yeastern Biotech, Taiwan, Republic of China). A total of 31 clones were subjected to sequence analysis, and the transcriptional start site of *rmpA* was determined from the longest DNA fragments.

Limiting-dilution RT-PCR. The reaction mixtures include primer sets RTrmpA01/RTrmpA02 or 23SR/23SF (Table 2) and the diluted cDNA templates from the first-strand synthesis in 5′-RACE PCR. The PCR program consisted of 30 cycles of 30 s at 94°C, 30 s at 50°C, and 20 s at 72°C. For a quantitative comparison of the *rmpA* expression levels, the intensity of the band resolved on agarose gel was analyzed and normalized with 23S rRNA gene by using ImageJ software (National Institutes of Health). The expression level of *rmpA* from the undiluted wild-type cDNA was set as 100.

Statistical analysis. A Student *t* test was used to determine the significance of the differences between the CPS amounts and the levels of β-galactosidase activity. The *P* values of <0.05 were considered statistically significant.

RESULTS

Expression of *rmpA* in *K. pneumoniae* CG43. On the basis of the sequence annotation, the DNA fragment containing the *rmpA2* gene with upstream *vagC* and *vagD* and downstream *iucABCDiutA* genes was labeled as PAI-1 (for pathogenicity island 1), while the *rmpA*-, *fecIRA*-, and *iroBCD*-containing region was named PAI-2 (Fig. 1A). The positive regulatory role of RmpA2 in the expression of the major virulence factor, CPS, has been demonstrated (20). However, whether RmpA plays a functional role remains unknown. PCR with a primer pair that could differentiate *rmpA* from *rmpA2* and Southern hybridization analysis were performed. As shown in Fig. 1B, the PCR products representing the *rmpA*-specific transcript could be detected using the reverse transcribed cDNA templates from *K. pneumoniae* CG43S3 or the Δ*rmpA2* mutant strain. This indicates that the *rmpA* on pLVPK is a functional gene and that the expression of *rmpA* is independent of RmpA2.

Deletion of *rmpA* reduced CPS production and virulence. To assess the functional role of RmpA, the *rmpA* deletion mutant was generated by using the allelic-exchange strategy. The colony of Δ*rmpA* mutant on the LB agar plate was found to be smaller than its parental strain, and the degree of mucoidy was reduced significantly, as determined by a string test (23), which refers to the ability to form a string when the bacterial colony was picked with toothpick. As shown in the sedimentation test in Fig. 2A, the Δ*rmpA* mutant, as well as the Δ*rcsB* mutant, could be rapidly precipitated by low-speed centrifugation. The loss of mucoid phenotype in the Δ*rmpA* mutant could be complemented with the transformation of pRK415-RmpA, or pRK415-RmpA2. Interestingly, the mucoid phenotype could not be restored by introducing the *rcsB* expression plasmid pRK415-RcsB. The sedimentation analysis also revealed that the introduction of pRK415-RmpA or pRK415-RmpA2 was able to increase the mucoviscosity of the *rmpA rmpA2* double mutant (Fig. 2A), indicating the independent regulatory activity of RmpA and RmpA2. The effect of *rcsB* deletion could only be complemented by transformation of the Δ*rcsB* mutant with pRK415-RcsB but not with pRK415-RmpA. As assessed by measuring the glucuronic acid content, which served as an indicator for *Klebsiella* K2 CPS (33), deletion of *rmpA* or *rcsB* caused a ca. 25% reduction in the amount of CPS compared to that of CG43S3 (Fig. 2B). The effect of *rmpA* or *rcsB* deletion could only be restored by transformation of Δ*rmpA* with pRK415-RmpA or transformation of Δ*rcsB* with pRK415-RcsB (Fig. 2C), which is consistent with the findings in Fig. 2A.

Furthermore, the *rmpA* deletion appeared to increase LD_{50} from 1×10^4 CFU to 5×10^5 CFU in the mouse peritonitis model and reduced the resistance to human serum from >95% to >70% (Table 3). The deficiency in serum resistance could be reverted by the introduction of pRK415-RmpA, suggesting a role of RmpA in bacterial virulence.

RmpA acted as an activator of *cps* expression. To investigate whether the CPS-deficient phenotype of Δ*rmpA* mutant was a result of altered expression of the *cps* genes, three reporter plasmids, pOrf12 ($P_{orf1\text{-}2}$::*lacZ*), pOrf315 ($P_{orf3\text{-}15}$::*lacZ*), and pOrf1617 ($P_{orf16\text{-}17}$::*lacZ*), each carrying a *lacZ* transcriptional fused to the putative promoter region of the K2 *cps* gene cluster (25), were used to transform *K. pneumoniae* strains CG43S3Δ*lacZ*, CG43S3Δ*rmpA*Δ*lacZ*, CG43S3Δ*rmpA2*Δ*lacZ*, or CG43S3Δ*rcsB*Δ*lacZ* individually. The promoter activity measurements shown in Fig. 3A reveal that the deletion of *rmpA* reduced the activity of $P_{orf1\text{-}2}$::*lacZ* and $P_{orf16\text{-}17}$::*lacZ*. A reduction in the activity $P_{orf1\text{-}2}$::*lacZ* or $P_{orf16\text{-}17}$::*lacZ* was also

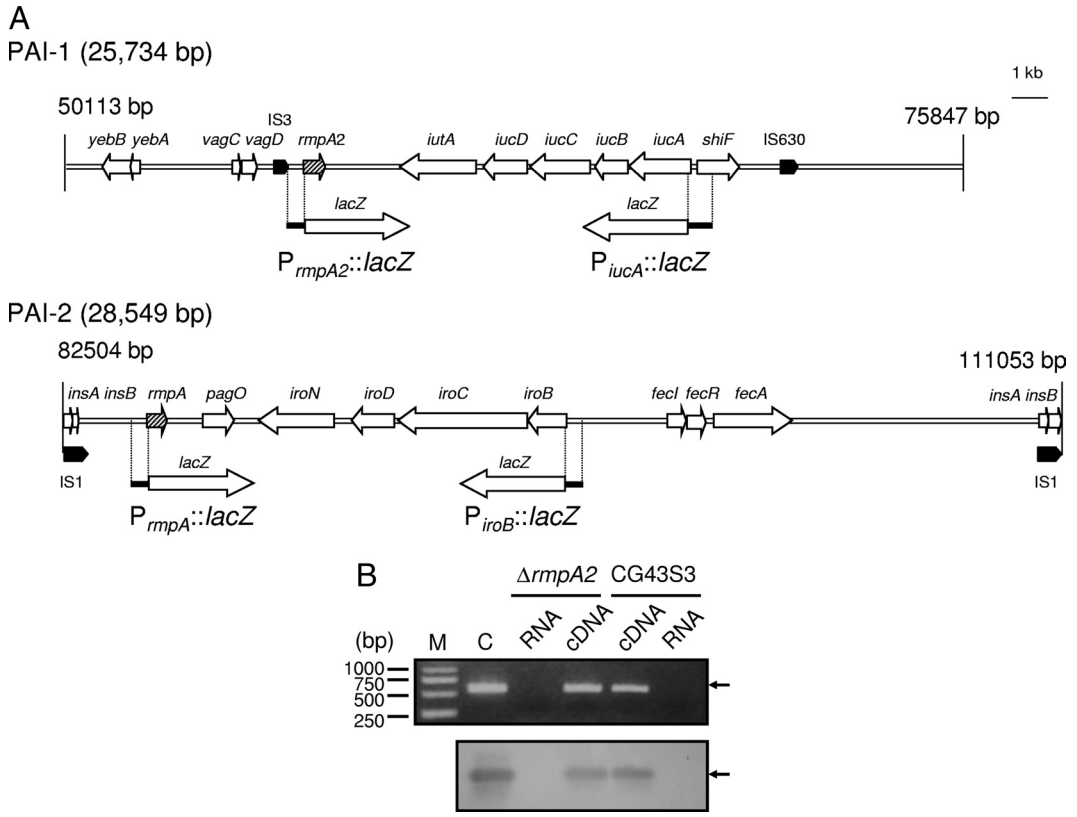

FIG. 1. Comparison of *rmpA* and *rmpA2* containing PAI-like regions and demonstration of *rmpA* expression. (A) The arrows indicate predicted open reading frames and insertion sequences. The reporter constructs used for promoter activity measurement are shown below. (B) Assessment of *rmpA* expression by PCR and Southern hybridization analysis. In the upper panel, the templates for the PCR include a plasmid carrying *rmpA* gene (lane C), the extracted total RNA or reverse-transcribed cDNA from *K. pneumoniae* CG43S3 (wild type) or *rmpA2* deletion mutant (Δ*rmpA2*). The lower panel shows the result of Southern blot analysis of the same gel with a probe specific to the *rmpA* gene; the arrow indicates the expected size of the PCR product.

observed in the Δ*rcsB* mutant. Interestingly, the deletion of *rmpA2* had less effect on the activity of $P_{orf16\text{-}17}$::*lacZ* compared to the *rmpA* deletion. As shown in Fig. 3B, the deleting effect of *rmpA*, *rmpA2*, or *rcsB* on $P_{orf3\text{-}15}$::*lacZ* activity was only apparent when the strains were grown in M9-glocuse minimal medium. Compared to that of *rmpA2*, the deletion of *rmpA* resulted in a more drastic reduction in the activity of $P_{orf1\text{-}2}$::*lacZ* and $P_{orf16\text{-}17}$::*lacZ* implying a differential regulation of RmpA and RmpA2 on the *cps* promoters. Nevertheless, the results suggested that the expression of RmpA, RcsB, and RmpA2 is required for *cps* expression.

RmpA regulates *cps* expression in an RcsB-dependent manner. To investigate the possibility of an interaction between RmpA and RcsB for *cps* expression, the *lacZ* reporter cassette on pOrf12 was cloned into a suicide vector, and the plasmid was mobilized into *K. pneumoniae* CG43S3Δ*lacZ*, CG43S3Δ*rmpA*Δ*lacZ*, or CG43S3Δ*rcsB*Δ*lacZ* individually. The resulting strain harboring a chromosomally integrated $P_{orf1\text{-}2}$::*lacZ* cassette was then transformed with different complementation plasmids, and the β-galactosidase activities were determined. As shown in Fig. 3C, the introduction of pRK415-RmpA or pRK415-RcsB could enhance $P_{orf1\text{-}2}$::*lacZ* activity in the parental strain, suggesting the functional activity of RmpA or RcsB. Functional RmpA could enhance *cps* expression in the *rmpA* deletion strain but not the *rcsB* deletion strain. Consistent with the phenotype observed in Fig. 2B, the functional RcsB carried by pRK415-RcsB could not restore *cps* expression in the *rmpA* deletion strain. The introduction of pRK415-RmpAN, which encoded a truncated RmpA without the carboxyl-terminal DNA binding region, into the *rmpA* deletion strain also failed to restore *cps* expression. The results suggest that RmpA activated *cps* expression in an RcsB-dependent manner and that its DNA-binding motif is required for regulation.

Analysis of interaction between RmpA and RcsB using two-hybrid analysis. Since the cooperation of RcsA and RcsB for regulation on K2 *cps* expression has been demonstrated (47), we thought of using EMSA to investigate whether the RmpA exerts RcsA-like activity to interact with RcsB in order to bind to the $P_{orf1\text{-}2}$ region cooperatively. However, the overproduction of RmpA using the pET expression system appeared to impair cell growth significantly; hence, the bacterial two-hybrid assay was used instead. Therefore, plasmids pTRG-RcsA, pTRG-RmpA, pTRG-RmpA2, pTRG-RmpAN, and pBT-RcsB, which harbored the λ-cI-RcsA, λ-cI-RmpA, λ-cI-RmpA2, λ-cI-RmpAN, and α-RNAP-RcsB coding sequences, respectively, were constructed. The interaction between α-RNAP and λ-cI fusion proteins would allow binding of λ-cI to the operator sequence and recruitment of α-RNAP to ini-

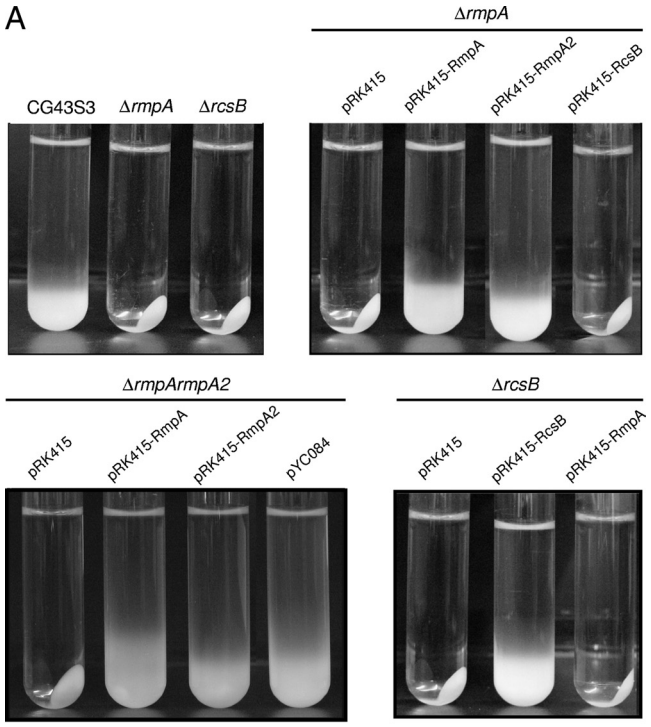

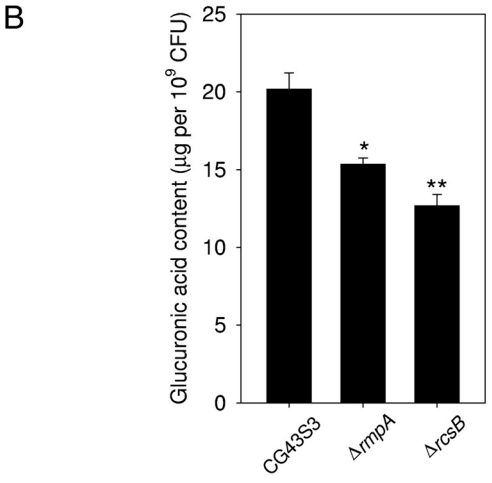

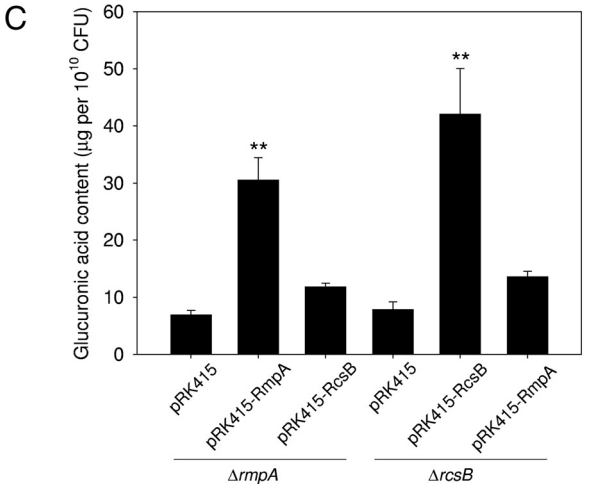

FIG. 2. Comparison of precipitation speeds and K2 CPS production in *K. pneumoniae* strains. (A) The strains tested were grown overnight in LB broth at 37°C and subjected to centrifugation at 4,000 × *g* for 5 min. (B) The glucuronic acid content, which served as an indicator of K2 CPS, was determined from overnight *K. pneumoniae* cultures. The results are expressed as the average of the triplicate samples. Error bars indicate standard deviations. *, $P < 0.01$; **, $P < 0.001$ compared to the parental strain CG43S3 ($n \geq 3$). (C) Quantification of *Klebsiella* K2 CPS production. The results are expressed as an average of triplicate samples. Error bars indicate standard deviations. **, $P < 0.001$ compared to the same strain carrying pRK415 ($n \geq 3$).

TABLE 3. Virulence properties of *K. pneumoniae* strains

Strain	LD_{50} (CFU)	Survival rate in human serum (%)[a]
CG43S3	1×10^4	95.6 ± 3.6
CG43S3Δ*rmpA*	5×10^5	71.2 ± 5.6
CG43S3Δ*rmpA*/pRK415-RmpA	ND[b]	>99
CG43S3Δ*galU* (control)	1×10^6	0

[a] The percent survival rate in human serum is expressed as 100 × (the number of viable bacteria after treatment with human serum/the number of viable bacteria after treatment with phosphate-buffered saline).
[b] ND, not determined.

tiate the transcription of both *ampR* and *lacZ* genes in the reporter cassette harbored in the *E. coli* reporter strain. The interaction between the recombinant proteins could be verified by bacterial growth on the X-Gal indicator plate supplemented with carbenicillin, and the level of interaction could be quantified by measuring the activation of the LacZ reporter.

As shown in Fig. 4A, the strain carrying pBT-RcsB/pTRG-RcsA or the positive control plasmids grew well on the indicator plate. Substitution of pBT-RcsB and pTRG-RcsA with pBT or pTRG resulted in poor or no growth. The strains carrying pBT-RcsB/pTRG-RmpA, pBT-RcsB/pTRG-RmpA2, or pBT-RcsB/pTRG-RmpAN also grew on the indicator plate (Fig. 4A). As shown in Fig. 4B, the strain carrying pBT-RcsB/pTRG-RcsA exhibited relatively higher activity than the strains carrying pBT-RcsB/pTRG-RmpA, pTRG-RmpA2, or pTRG-RmpAN. The transformants harboring pBT-RcsB and pTRG-RmpA, pTRG-RmpA2, or pTRG-RmpAN also exhibited higher activity compared to strains wherein which pBT-RcsB was replaced by pBT (Fig. 4B, right panel). The results suggested an *in vivo* interaction between RcsB and RmpA, and the N-terminal peptide (residues 1 to 84) of RmpA may play an important role in the interaction.

Coimmunoprecipitation analysis of the interaction between RmpA and RcsB. To confirm the results from the two-hybrid analysis, coimmunoprecipitation was also performed. The full-length RcsA, RmpA, RmpA2, and RmpAN coding regions were cloned into pGEX-5X-1 to generate plasmids pGST-RcsA, pGST-RmpA, pGST-RmpA2, and pGST-RmpAN, respectively. The plasmid pACYC184-RcsB, which is compatible with pGEX-5X-1, was also constructed. Using anti-GST or anti-His monoclonal antibody, the amounts of the recombinant GST fusion proteins and the recombinant RcsB in the Pre-IP samples were determined (Fig. 5A). As shown in Fig. 5B, the immunoprecipitates of pGEX-RcsA/pACYC184-RcsB, pGEX-

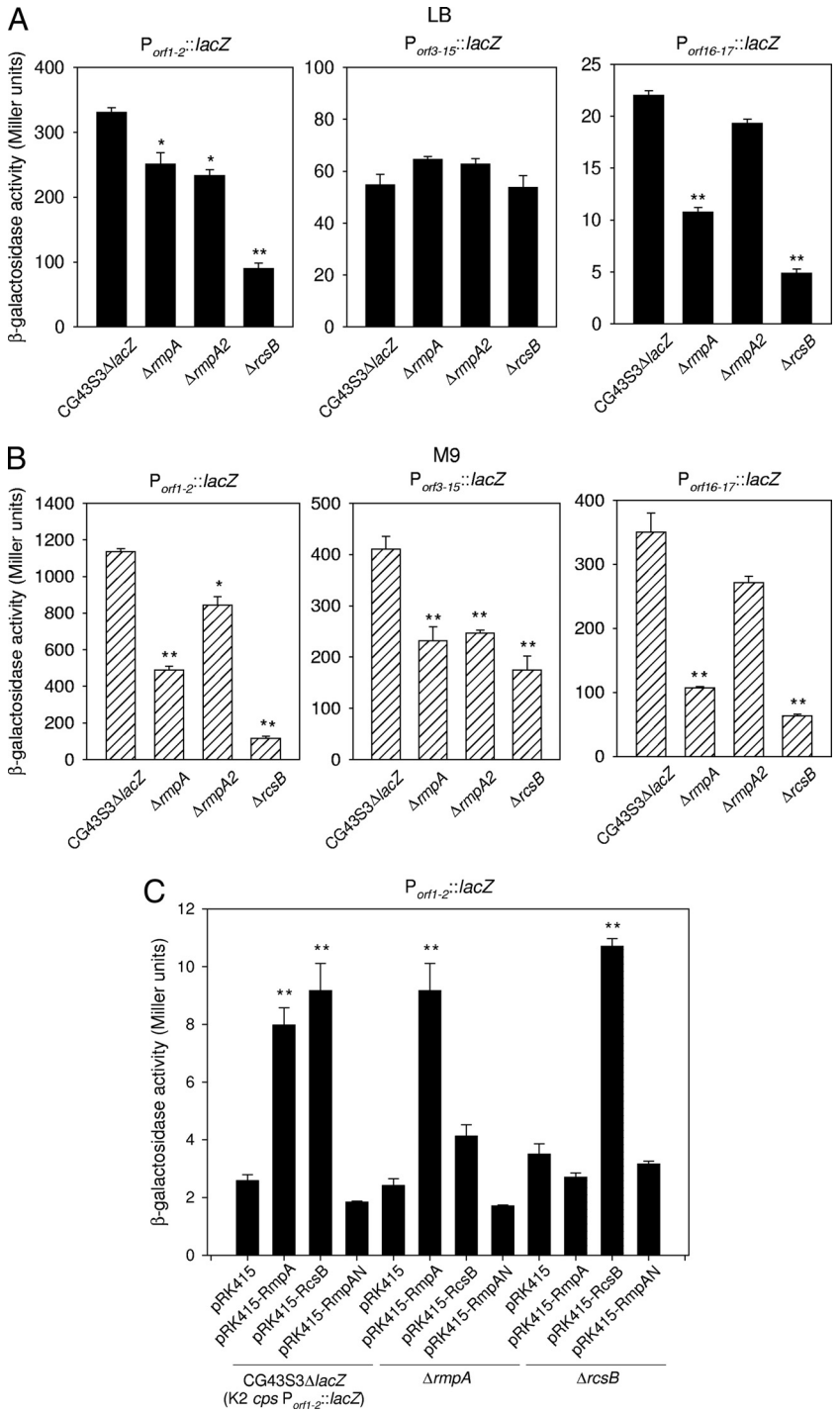

FIG. 3. Expression of K2 *cps* genes in various genetic backgrounds. The β-galactosidase activities of K2 *cps* $P_{orf1\text{-}2}$::*lacZ*, $P_{orf3\text{-}15}$::*lacZ*, and $P_{orf16\text{-}17}$::*lacZ* in *K. pneumoniae* CG43S3Δ*lacZ* (wild-type) and its isogenic strains (Δ*rmpA*Δ*lacZ*, Δ*rmpA2*Δ*lacZ*, and Δ*rcsB*Δ*lacZ*) harboring each of the reporter plasmids pOrf12, pOrf315, or pOrf1617 were determined from log-phase cultures grown in LB broth (A) or M9-glucose medium (B). The results are shown as an average of triplicate samples. Error bars indicate standard deviations. *, $P < 0.01$; **, $P < 0.001$ compared to the parental strain CG43S3Δ*lacZ* ($n \geq 3$). (C) The *K. pneumoniae* CG43S3Δ*lacZ* (wild-type) and its isogenic strains (Δ*rmpA*Δ*lacZ* and Δ*rcsB*Δ*lacZ*), each carrying a chromosomally integrated K2 *cps* $P_{orf1\text{-}2}$::*lacZ* cassette, were transformed individually with pRK415 and its derived plasmids. The β-galactosidase activities were determined from log-phase (OD_{600} of 0.7) cultures grown in LB broth. The results are shown as the average of the triplicate samples. Error bars indicate standard deviations. **, $P < 0.001$ compared to each strain carrying pRK415 ($n \geq 3$).

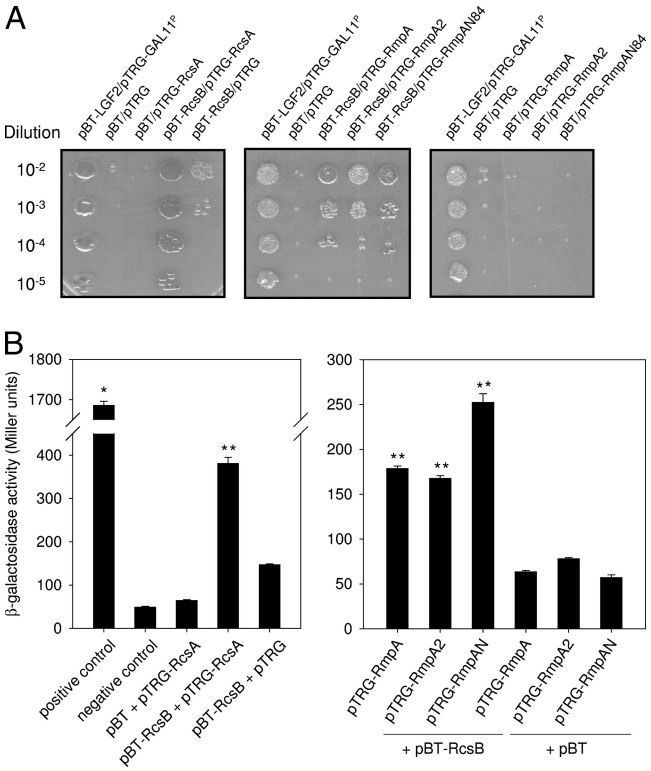

FIG. 4. Bacterial two-hybrid analysis of the interaction between RcsA/RcsB, RcsB/RmpA, and RcsB/RmpA2 proteins. (A) The growth of serially diluted cultures of *E. coli* reporter strains cotransformed with pTRG and pBT or the derived plasmids was investigated on the indicator plate. (B) The *E. coli* reporter strains cotransformed with pTRG and pBT or the derived plasmids were grown to log phase (OD_{600} of 0.5) in LB broth and induced with IPTG, and the β-galactosidase activities were determined. The results are shown as the average of the triplicate samples. Error bars indicate standard deviations. *, $P < 0.0001$ compared to negative control strain carrying the bait vector pBT and the target vector pTRG ($n \geq 3$). **, $P < 0.001$ compared to the strain carrying the bait vector pBT ($n \geq 3$).

RmpA/pACYC184-RcsB, pGEX-RmpAN/pACYC184-RcsB, or pGEX-RmpA2/pACYC184-RcsB pulled down with the glutathione-Sepharose all contained the RcsB-His_6, as determined by using anti-His monoclonal antibody or anti-RcsB polyclonal antibody. The amounts of recombinant RcsB protein precipitated by GST-RcsA and GST-RmpA were much lower than those pulled down by GST-RmpAN and GST-RmpA2 (Fig. 5B). This may have resulted from instability of the GST-RcsA and GST-RmpA fusion proteins, as reflected by very low amounts of both proteins obtained after IP (data not shown). The results further supported a role of RmpA or RmpA2 as an auxiliary factor, like RcsA, for RcsB in regulating the CPS biosynthesis.

The expression of *rmpA* is subjected to negative regulation by Fur. Differential control likely explains the coexistence of the two functional mucoid factors, RmpA and RmpA2, in the *cps* expression in the bacteria. To verify this, the DNA fragments encompassing the putative promoter region of *rmpA* or *rmpA2* was cloned in front of the promoterless *lacZ* to generate placZ15-PrmpA and placZ15-PrmpA2. The resulting plasmids were then transformed individually into *K. pneumoniae* CG43S3Δ*lacZ* for promoter activity measurements. In contrast to the negative autoregulation for *rmpA2* expression (23), the *rmpA* expression appeared to be independent of autoregulatory control (data not shown).

Since *rmpA* and *rmpA2* are, respectively, located next to the iron acquisition genes *iucABCD*, *iutA*, and *iroBCDN* (Fig. 1A), we sought to determine whether any iron uptake regulator is involved in their expression. A close inspection of the *rmpA* and *rmpA2* upstream regions revealed a Fur box-like sequence (2, 11) on P_{rmpA} but not on P_{rmpA2}. This element was also identified in front of a set of Fur-regulated genes including *iucABCD*, *iroBCD*, *feoAB*, and *fur* (data not shown). To investigate whether Fur, the global regulator for iron uptake regulation, participated in the control of the gene expression, the expression levels of P_{rmpA}::*lacZ* and P_{rmpA2}::*lacZ* were measured in the wild-type strain and in the *fur* deletion mutant. As shown in Fig. 6A, *fur* deletion resulted in a higher level of activity for the Fur-dependent promoters P_{iucA} and P_{iroB} in LB medium. An increased level of P_{rmpA}::*lacZ* expression in the Δ*fur* mutant was even more profound when the bacterial culture was switched from LB medium to the M9-glucose medium (Fig. 6B). In the presence of iron scavenger 2,2-dipyridyl, the activity of P_{iucA}::*lacZ*, P_{iro}::*lacZ*, or P_{rmpA}::*lacZ* was higher in M9-glucose medium but less affected by Fur. On the other hand, the deletion of *fur* or the addition of iron scavenger had no apparent effect on the expression of P_{rmpA2}::*lacZ* in either medium (Fig. 6). The results suggest that Fur negatively regulate the expression of P_{rmpA} but does not participate in the regulation of *rmpA2* expression.

The recombinant Fur was able to bind specifically to P_{rmpA}. The Fur box-like sequence could be predicted upstream of *iucA*, *iroB*, and *rmpA*, as shown in Fig. 7A. To further ascertain the effect of Fur on *rmpA* expression, an EMSA was performed. The DNA fragments encompassing P_{iucA} (P1), P_{iroB} (P2), and P_{rmpA} (P3) and the truncated forms P4, P5, and P6, as depicted in Fig. 7A, were isolated and isotope labeled for the analysis. As shown in Fig. 7B, the purified recombinant His_6-Fur protein was able to bind to the DNA probes P1, P2, and P3. By using different lengths of P_{rmpA}, the binding of His_6-Fur could be observed for P3, P4, and P5 but not for P6 (Fig. 7C). This suggested that the His_6-Fur binding site may be located between −226 to −184 relative to the RmpA start codon (Fig. 7A). As shown in Fig. 7D, the formation of the P_{rmpA}/Fur complex could be observed as the amount of His_6-Fur increased, and the binding specificity was demonstrated as the complex diminished in the presence of excess nonlabeled P3 or P5 acting as specific competitor DNA. The binding of His_6-Fur on P_{rmpA} remained unaffected by the addition of excess amounts of pT7-7 (42), a plasmid without a Fur box-containing sequence, pUC19 DNA, *rmpA* gene, or P6 DNA fragment. The results support the conclusion that the recombinant Fur protein could specifically interact with P_{rmpA} DNA.

Identification of *rmpA* transcriptional start site. As shown in Fig. 8A, a single DNA band has been obtained from the 5′-RACE analysis using either primer pair. Sequence analysis of a total of 31 clones revealed the transcription start site at the G nucleotide at position −80 relative to the translational start site of RmpA. As shown in Fig. 8B, a conserved −10 and −35 promoter sequence of σ^{70} could be readily identified. Limiting-dilution RT-PCR was subsequently carried out to determine whether the *rmpA* tran-

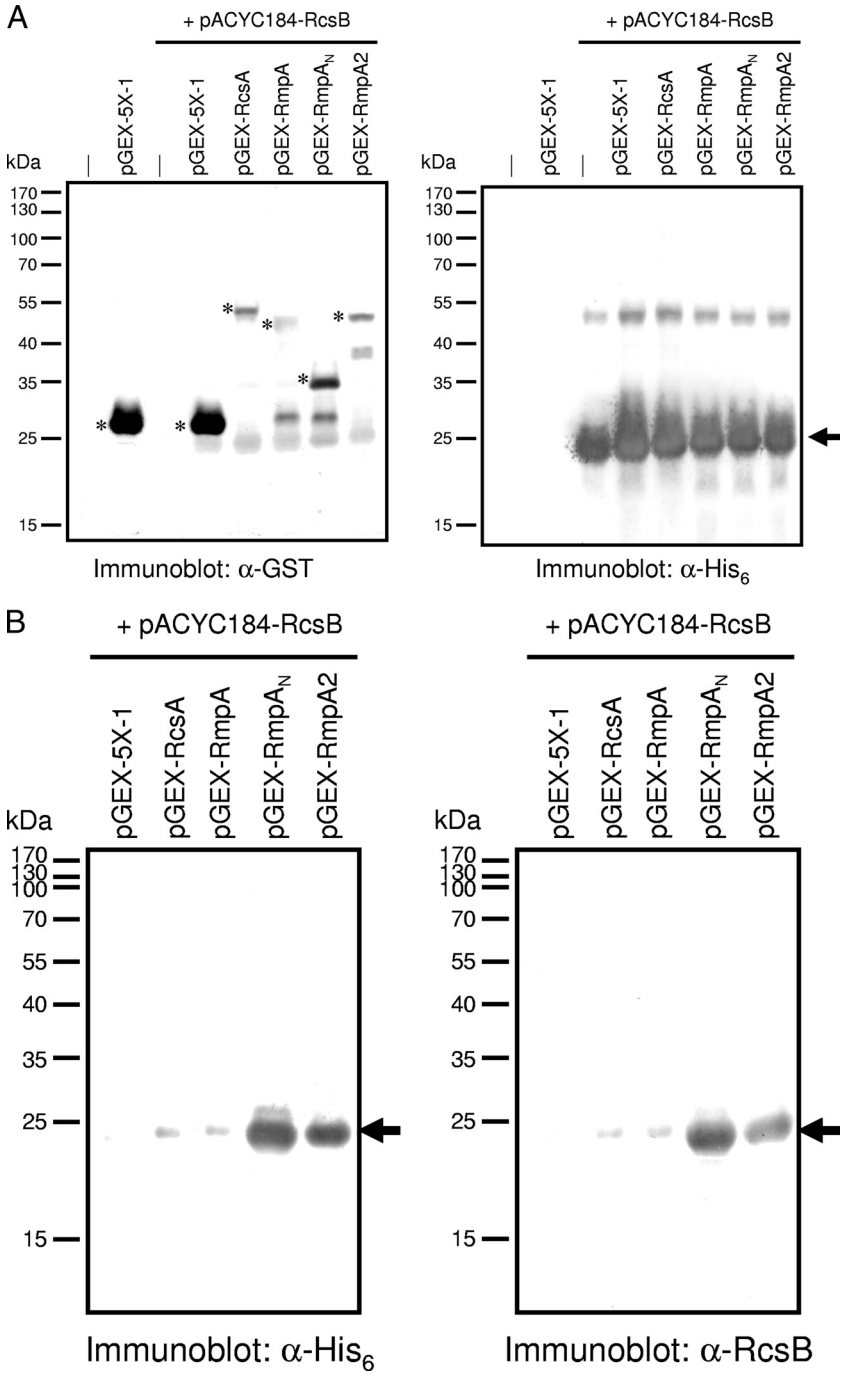

FIG. 5. Coimmunoprecipitation analysis of the interaction between RcsA/RcsB, RcsB/RmpA, and RcsB/RmpA2 proteins. (A) Results of immunoblot analysis of Pre-IP samples using anti-GST (α-GST) or anti-His$_6$ (α-His$_6$) monoclonal antibodies showing, respectively, the expression of GST fusion proteins and RcsB-His$_6$. Samples were supernatants of induced bacterial cell lysates prepared from *E. coli* BL21(DE3) with or without (–) different combinations of expression vectors as indicated above the figure, and 10 μg of total protein was loaded in each well. The asterisks indicate the expected size of GST and GST fusion proteins. The arrow indicates the expected size of RcsB-His$_6$. (B) Results of immunoblot analysis of IP samples showing the interaction between the recombinant proteins. Protein complexes were precipitated with glutathione-Sepharose beads, separated by SDS-PAGE, and immunoblotted with anti-His$_6$ (α-His$_6$) monoclonal antibody or anti-RcsB-His$_6$ (α-RcsB) polyclonal antiserum. The arrows indicate the expected size of RcsB-His$_6$.

scription would be affected by Fur. As shown in Fig. 8C, a stronger signal for *rmpA* transcript in the *fur* mutant than in the parental strain also supports a negative regulatory role of Fur on the *rmpA* expression.

Deletion of *fur* led to overproduction of CPS. If *rmpA* expression is negatively regulated by Fur, then the CPS level in the *fur* deletion mutant should increase. As shown in Fig. 9A, the Δ*fur* mutant formed more mucoid and glistening colonies

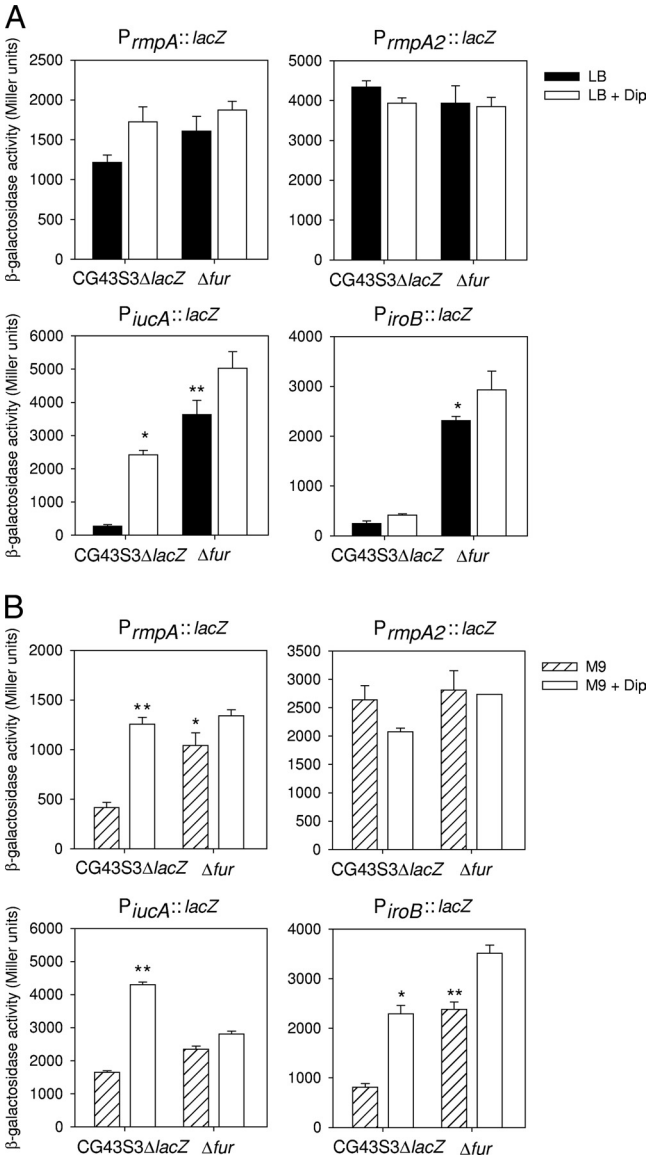

FIG. 6. Effect of *fur* deletion or iron depletion on the activity of P_{rmpA}::*lacZ*, P_{rmpA2}::*lacZ*, P_{iucA}::*lacZ*, and P_{iroB}::*lacZ*. The β-galactosidase activities of *K. pneumoniae* CG43S3Δ*lacZ* (wild type) or its isogenic *fur* deletion mutant (Δ*fur*) carrying, respectively, placZ15-PrmpA (P_{rmpA}::*lacZ*), placZ15-PrmpA2 (P_{rmpA2}::*lacZ*), placZ15-PiucA (P_{iucA}::*lacZ*), or placZ15-PiroB (P_{iroB}::*lacZ*) were determined from cultures grown in LB (A) or M9-glucose (B) medium. The media were supplemented with (white bars) or without (black bars and striped bars) 0.2 mM iron chelator 2,2-dipyridyl (+Dip). The results are shown as the average of the triplicate samples. Error bars indicate the standard deviations. *, $P < 0.01$; **, $P < 0.001$ compared to the parental strain CG43S3Δ*lacZ* grown in media without supplements ($n \geq 3$).

compared to the parental strain. In a string test, the Δ*fur* mutant could form a string at least 3-fold longer than its parental strain (data not shown). Introduction of pRK415-Fur carrying a functional *fur* allele in Δ*fur* mutant resulted in small colonies (Fig. 9A) and a readily precipitated phenotype (Fig. 9B). The changes in CPS production were also evident in the glucuronic acid content measurement. As shown in Fig. 9C, the *fur* mutant exhibited a >2-fold increase in the glucuronic acid production, while transformation with pRK415-Fur resulted in an ca. 50% reduction of the glucuronic acid.

DISCUSSION

The presence of *rmpA* and *rmpA2* on pLVPK as two independent loci 29 kb apart has been demonstrated (8). As shown in Fig. 1A, the DNA fragments containing *rmpA2* and *rmpA* also harbored an iron acquisition gene cluster and insertion sequence, which are characteristics of a pathogenicity island, and hence named PAI-1 and PAI-2, respectively. Why and how the evolutionary convergence of the similar gene organization occurred remained to be explained. In the present study, we show that *rmpA* and *rmpA2* genes are present in one bacterial strain and that both encode a mucoid factor contributing to K2 CPS biosynthesis. Presumably, differential control on the expression of these two mucoid factors is required for an efficient regulatory function with no redundant activity in the bacteria.

Sequence analysis revealed that RmpA and RmpA2 belong to the UhpA-LuxR family of transcription factors, which also include RcsA and RcsB (41). The involvement of RcsB in *Klebsiella* K2 capsule biosynthesis of the recombinant *E. coli* K-12 has been demonstrated (44). Previous studies have found that RcsB must interact with RcsA to form a heterodimer in order to bind specifically to the *cps* promoter for transcription initiation (21). In *E. coli*, the cellular level of RcsA was limited at 37°C due to its degradation by the Lon protease, and thus the colonic acid capsule was overproduced only at lower temperatures (16). In *K. pneumoniae* CG43, however, a profound production of CPS was observed at 37°C. We assumed that RmpA or RmpA2 could take the place of RcsA to regulate the *cps* expression at 37°C. This hypothesis was supported by the fact that the deletion of *rcsA* in *K. pneumoniae* CG43 did not affect the mucoid phenotype or the CPS amount at 37°C (data not shown). Moreover, the two-hybrid analysis and coimmunoprecipitation assay further demonstrated that RmpA or RmpA2, in addition to RcsA, was able to interact with RcsB. Therefore, in *K. pneumoniae*, multiple accessory factors may be used in order to increase the CPS biosynthesis in response to different environmental stimuli.

A conserved RcsAB box sequence has been identified in *Klebsiella* K2 *cps* $P_{orf1\text{-}2}$ (47), and analysis of the $P_{orf16\text{-}17}$ sequence also revealed a semiconserved RcsAB box. This suggested that the decrease of the CPS production in the Δ*rmpA* mutant may have been due to a reduction in the expression of *cps-orf1-2* and *cps-orf16-17*. The existence of an *rmpA* gene has been correlated to the hypermucoviscosity phenotype in *K. pneumoniae* clinical isolates (51). It is interesting that no *rmpA* homologue in any other bacterial genomes could be identified. The BLAST (http://www.ncbi.nlm.nih.gov) search in the released genome sequences of *K. pneumoniae* NTUH-K2044 (49), MGH78578 (http://genome.wustl.edu/), and 342 (14) revealed the presence of *rmpA* only in NTUH-K2044, which is a heavy encapsulated clinical isolate of K1 serotype (12, 51). We have also observed that *rmpA* was more prevalent in the strains belonging to K1/K2 serotypes (36 out of 36 isolates [100%]) than in the non-K1/K2 clinical isolates (28 out of 83 isolates [33.73%]) collected in our laboratory. The presence of *rmpA* in *K. pneumoniae* K1 or K2 isolates has also been associated with virulence in mice (4). These findings suggest that the profound

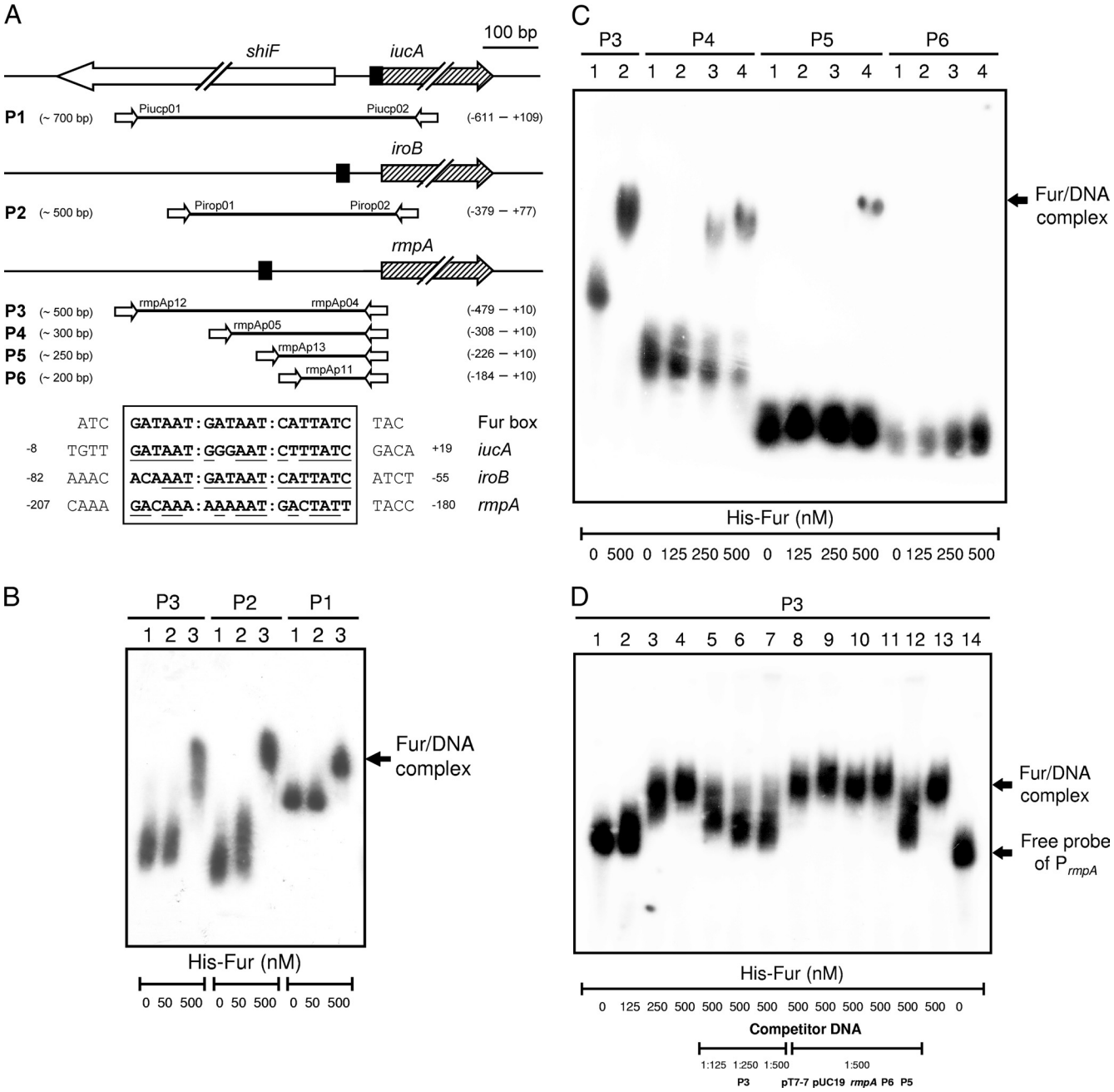

FIG. 7. EMSA of the recombinant His_6-Fur and its target promoters. (A) Diagrammatic representation of the *iucA*, *iroB*, and *rmpA* loci. The large arrows represent the open reading frames. The relative positions of the primer sets used in PCR amplification of the DNA probes are, respectively, indicated, and the numbers denote the relative positions to the translational start site. Names and sizes of the DNA probes are shown on the left. The dashed boxes indicate the predicted Fur binding sequences, and the alignment result is shown below. (B) Binding of His_6-Fur to its target promoters. The ^{32}P-labeled DNA probes of P_{iucA} (P1), P_{iroB} (P2), and P_{rmpA} (P3) were incubated with increasing amounts of recombinant His_6-Fur protein as indicated. (C) Binding of His_6-Fur to P_{rmpA}. The ^{32}P-labeled DNA probes of P_{rmpA} (P3, P4, P5, and P6) were incubated with increasing amounts of recombinant His_6-Fur protein as indicated. (D) Binding specificity of His_6-Fur to P_{rmpA}. The ^{32}P-labeled DNA probe of P_{rmpA} (P3) was incubated with various amounts of His_6-Fur as indicated. Binding specificity was investigated by adding indicated amounts of unlabeled specific (P3 and P5, lanes 5 to 7 and lane 12) or nonspecific (pT7-7, pUC19 plasmid DNA, *rmpA* gene, and P6, lanes 8 to 11) competitor DNA fragments.

expression of *K. pneumoniae* CPS, which is a major virulence factor, could be attributed to the regulation by RmpA or its homologue.

Similar to *rmpA2*, *rmpA* harbored a poly(G) tract in the coding sequence. The occurrence of DNA slip-strand synthesis may result in a truncated RmpA of abnormal function. Conceivably, the frequency of the mutation caused by DNA slip-strand synthesis in *rmpA* or *rmpA2* may play a role in the differential expression of the two regulatory genes. A Fur-box-like sequence was identified within −146 and −104 upstream

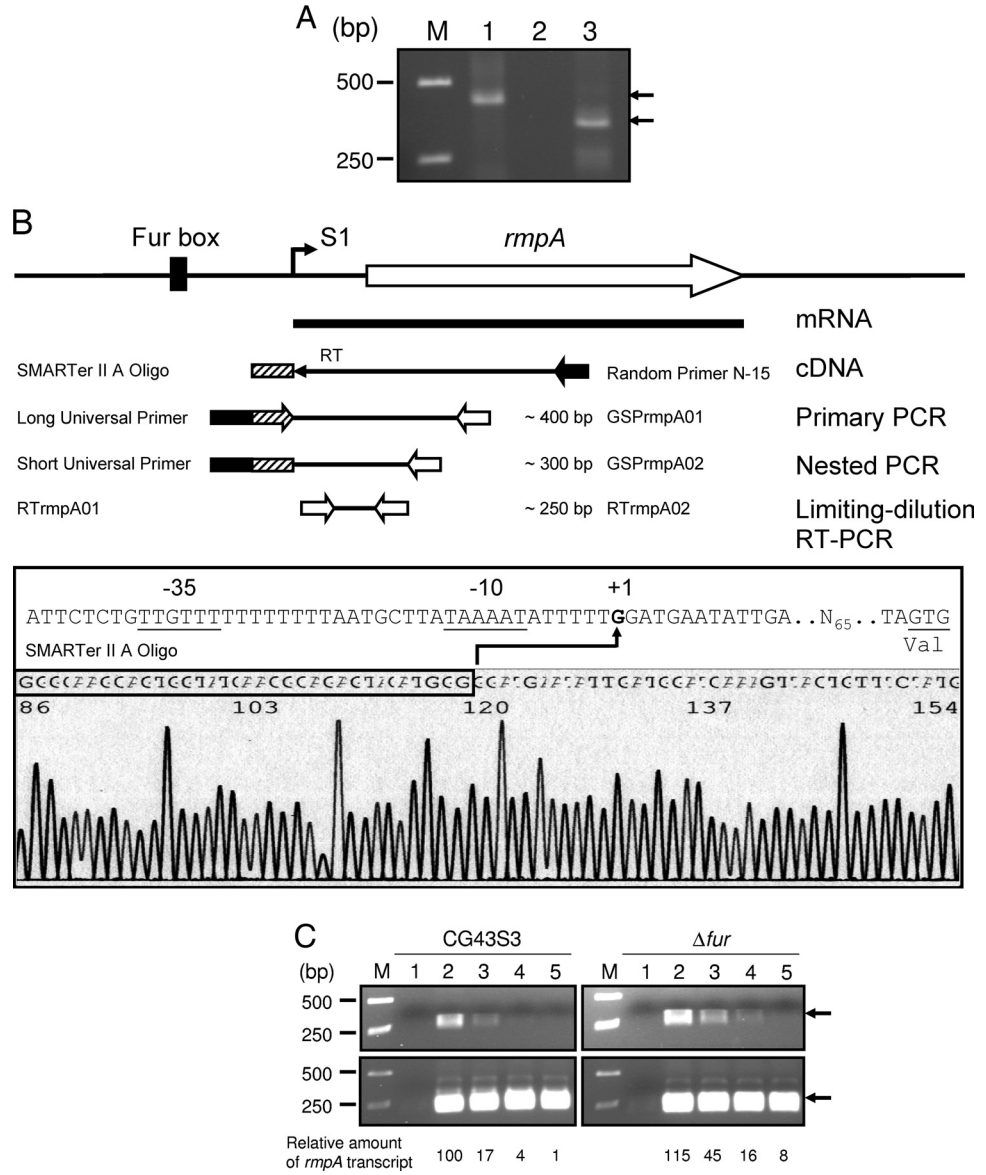

FIG. 8. Identification of *rmpA* transcription start site by 5′-RACE. (A) Electrophoresis of the 5′-RACE PCR products. M, DNA ladder. The templates used in each PCR include the cDNA from *K. pneumoniae* CG43S3 (primary PCR) (lane 1), reverse transcription reaction mixture without transcriptase as a negative control (lane 2), or 100-fold-diluted primary PCR mixture (nested PCR) (lane 3). The arrows indicate the expected sizes of the PCR products. (B) Schematic representation of the *rmpA* locus and the 5′-RACE experimental design. The large arrow represents the RmpA open reading frame. The relative positions of the primers and expected sizes of the products in the primary and nested PCRs are indicated. The *rmpA* transcriptional start site is marked as S1. The potential −10 and −35 sites and the translational start site are underlined. (C) Assessment of *rmpA* transcription by limiting-dilution RT-PCR. The templates used in each reaction include total RNA (lane 1) and the 4-fold serially diluted cDNA (lanes 2 to 5 represent, respectively 1-, 1/4-, 1/16-, and 1/64-fold dilutions) from *K. pneumoniae* CG43S3 or its isogenic *fur* mutant. The upper panel shows the results of electrophoresis of the RT-PCR products amplified with primers RTrmpA01/RTrmpA02. The RT-PCR products using 23S rRNA gene primers are shown in the lower panel. The expression levels of *rmpA* were quantified and normalized with 23S rRNA using ImageJ software (National Institutes of Health) as shown below. The *rmpA* expression level of the undiluted cDNA from *K. pneumoniae* CG43S3 was set as 100. The arrows indicate the expected size of the PCR products. M, DNA ladder.

of the transcription start site (Fig. 8B). This site was not uncommon compared to a genome-wide study in *Yersinia pestis* (15), in which 17 of 34 predicted Fur binding sites were located at −100 relative to each transcriptional start site. Also, as shown in Fig. 8C, the *rmpA* transcript was increased upon the deletion of *fur*, indicating a negative regulation of Fur on *rmpA* expression in *K. pneumoniae*.

Fur governs iron uptake by repressing the transcription of the genes involved in the biosynthesis of siderophore, iron storage, iron sparing, and respiration (2, 24, 43). In addition, it is also involved in virulence properties (46, 50), acid stress response (13), osmotic shock (17), and chemotaxis (10). In the present study, a negative role of Fur in CPS biosynthesis that is achieved by the reduction of the RmpA expression is re-

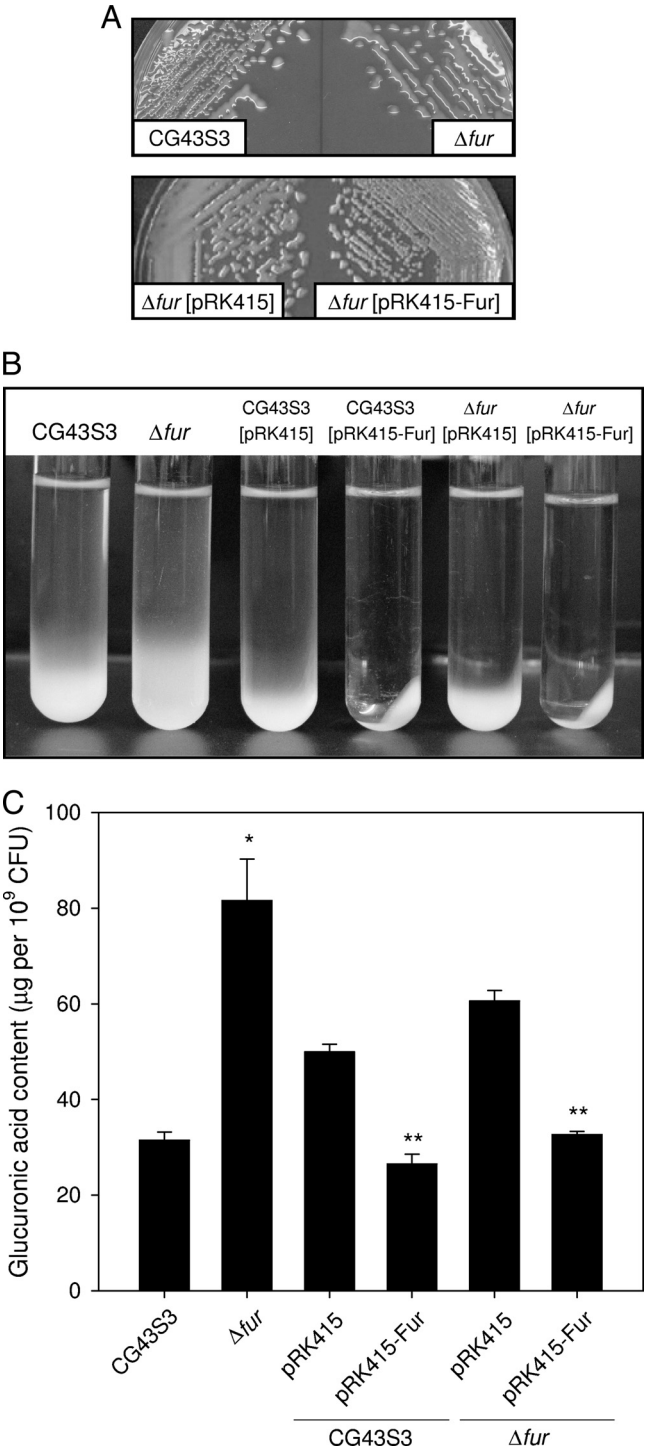

FIG. 9. Phenotype comparison of *K. pneumoniae* CG43S3, the *fur* deletion mutant, and the complemented strain. (A) The bacterial strains on LB agar plates incubated at 37°C for 48 h. (B) Sedimentation test and quantification of K2 CPS for strains grown overnight in LB broth at 37°C and subjected to centrifugation at 4,000 × *g* for 5 min. (C) The glucuronic acid contents (μg/10^9 CFU) determined from overnight *K. pneumoniae* cultures, expressed as the average of the triplicate samples ± the standard deviations. *, $P < 0.001$ compared to the parental strain CG43S3 ($n \geq 3$). **, $P < 0.001$ compared to each strain carrying pRK415 ($n \geq 3$).

ported for the first time. The findings imply that some *K. pneumoniae* strains may face iron shortage during infection; accordingly, the genes involved in both the biosynthesis of the iron acquisition system and the production of CPS are upregulated. Therefore, coordination between CPS production and iron uptake may play an important role in the pathogenesis of the bacteria. Nevertheless, *cps* expression was also subjected to regulation by the 2CS response regulators KvgA, KvhA, and KvhR (26). How the interplay between Fur, RmpA, and the 2CS determines the control of the *cps* expression remains to be elucidated.

In summary, our results indicate that in *K. pneumoniae* CG43, the mucoid factor RmpA exerts a regulatory role on *cps* expression in an RcsB-dependent manner. The *fur* deletion increased *rmpA* expression but had no effect on *rmpA2* expression. In addition, the recombinant Fur could bind specifically to the putative promoter of *rmpA*. This suggests that Fur plays a role in the differential expression of RmpA and RmpA2. This is also the first report that investigates the role of *Klebsiella* Fur in the regulation of CPS biosynthesis.

ACKNOWLEDGMENTS

The study is supported by grants from the Veterans General Hospital/Taiwan University System (VGHUST94-P5-27), the National Research Program for Genome Medicine (NSC96-3112-B009-001), and the National Science Council (97-2320-B-009-001-MY3).

REFERENCES

1. **Arakawa, Y., R. Wacharotayankun, T. Nagatsuka, H. Ito, N. Kato, and M. Ohta.** 1995. Genomic organization of the *Klebsiella pneumoniae* cps region responsible for serotype K2 capsular polysaccharide synthesis in the virulent strain Chedid. J. Bacteriol. **177:**1788–1796.
2. **Baichoo, N., and J. D. Helmann.** 2002. Recognition of DNA by Fur: a reinterpretation of the Fur box consensus sequence. J. Bacteriol. **184:**5826–5832.
3. **Brill, J. A., C. Quinlan-Walshe, and S. Gottesman.** 1988. Fine-structure mapping and identification of two regulators of capsule synthesis in *Escherichia coli* K-12. J. Bacteriol. **170:**2599–2611.
4. **Brisse, S., C. Fevre, V. Passet, S. Issenhuth-Jeanjean, R. Tournebize, L. Diancourt, and P. Grimont.** 2009. Virulent clones of *Klebsiella pneumoniae*: identification and evolutionary scenario based on genomic and phenotypic characterization. PLoS One **4:**e4982.
5. **Campos, M. A., M. A. Vargas, V. Regueiro, C. M. Llompart, S. Alberti, and J. A. Bengoechea.** 2004. Capsule polysaccharide mediates bacterial resistance to antimicrobial peptides. Infect. Immun. **72:**7107–7114.
6. **Chang, A. C., and S. N. Cohen.** 1978. Construction and characterization of amplifiable multicopy DNA cloning vehicles derived from the P15A cryptic miniplasmid. J. Bacteriol. **134:**1141–1156.
7. **Chang, H. Y., J. H. Lee, W. L. Deng, T. F. Fu, and H. L. Peng.** 1996. Virulence and outer membrane properties of a galU mutant of *Klebsiella pneumoniae* CG43. Microb. Pathog. **20:**255–261.
8. **Chen, Y. T., H. Y. Chang, Y. C. Lai, C. C. Pan, S. F. Tsai, and H. L. Peng.** 2004. Sequencing and analysis of the large virulence plasmid pLVPK of *Klebsiella pneumoniae* CG43. Gene **337:**189–198.
9. **Domenico, P., S. Schwartz, and B. A. Cunha.** 1989. Reduction of capsular polysaccharide production in *Klebsiella pneumoniae* by sodium salicylate. Infect. Immun. **57:**3778–3782.
10. **Ernst, F. D., S. Bereswill, B. Waidner, J. Stoof, U. Mader, J. G. Kusters, E. J. Kuipers, M. Kist, A. H. van Vliet, and G. Homuth.** 2005. Transcriptional profiling of *Helicobacter pylori* Fur- and iron-regulated gene expression. Microbiology **151:**533–546.
11. **Escolar, L., J. Perez-Martin, and V. de Lorenzo.** 1999. Opening the iron box: transcriptional metalloregulation by the Fur protein. J. Bacteriol. **181:**6223–6229.
12. **Fang, C. T., Y. P. Chuang, C. T. Shun, S. C. Chang, and J. T. Wang.** 2004. A novel virulence gene in *Klebsiella pneumoniae* strains causing primary liver abscess and septic metastatic complications. J. Exp. Med. **199:**697–705.
13. **Foster, J. W., and H. K. Hall.** 1992. Effect of *Salmonella typhimurium* ferric uptake regulator (*fur*) mutations on iron- and pH-regulated protein synthesis. J. Bacteriol. **174:**4317–4323.
14. **Fouts, D. E., H. L. Tyler, R. T. DeBoy, S. Daugherty, Q. Ren, J. H. Badger, A. S. Durkin, H. Huot, S. Shrivastava, S. Kothari, R. J. Dodson, Y. Moham-**

oud, H. Khouri, L. F. Roesch, K. A. Krogfelt, C. Struve, E. W. Triplett, and B. A. Methe. 2008. Complete genome sequence of the N2-fixing broad host range endophyte *Klebsiella pneumoniae* 342 and virulence predictions verified in mice. PLoS Genet. **4:**e1000141.

15. **Gao, H., D. Zhou, Y. Li, Z. Guo, Y. Han, Y. Song, J. Zhai, Z. Du, X. Wang, J. Lu, and R. Yang.** 2008. The iron-responsive Fur regulon in *Yersinia pestis*. J. Bacteriol. **190:**3063–3075.
16. **Gottesman, S., and V. Stout.** 1991. Regulation of capsular polysaccharide synthesis in *Escherichia coli* K12. Mol. Microbiol. **5:**1599–1606.
17. **Hoffmann, T., A. Schutz, M. Brosius, A. Volker, U. Volker, and E. Bremer.** 2002. High-salinity-induced iron limitation in *Bacillus subtilis*. J. Bacteriol. **184:**718–727.
18. **Hsu, J. L., H. C. Chen, H. L. Peng, and H. Y. Chang.** 2008. Characterization of the histidine-containing phosphotransfer protein B-mediated multistep phosphorelay system in *Pseudomonas aeruginosa* PAO1. J. Biol. Chem. **283:** 9933–9944.
19. **Huang, Y. H., L. Ferrieres, and D. J. Clarke.** 2006. The role of the Rcs phosphorelay in *Enterobacteriaceae*. Res. Microbiol. **157:**206–212.
20. **Keen, N. T., S. Tamaki, D. Kobayashi, and D. Trollinger.** 1988. Improved broad-host-range plasmids for DNA cloning in gram-negative bacteria. Gene **70:**191–197.
21. **Kelm, O., C. Kiecker, K. Geider, and F. Bernhard.** 1997. Interaction of the regulator proteins RcsA and RcsB with the promoter of the operon for amylovoran biosynthesis in Erwinia amylovora. Mol. Gen. Genet. **256:**72–83.
22. **Lahiri, S., L. Pulakat, and N. Gavini.** 2005. Functional NifD-K fusion protein in Azotobacter vinelandii is a homodimeric complex equivalent to the native heterotetrameric MoFe protein. Biochem. Biophys. Res. Commun. **337:**677–684.
23. **Lai, Y. C., H. L. Peng, and H. Y. Chang.** 2003. RmpA2, an activator of capsule biosynthesis in *Klebsiella pneumoniae* CG43, regulates K2 cps gene expression at the transcriptional level. J. Bacteriol. **185:**788–800.
24. **Lee, J. W., and J. D. Helmann.** 2007. Functional specialization within the Fur family of metalloregulators. Biometals **20:**485–499.
25. **Lin, C. T., T. Y. Huang, W. C. Liang, and H. L. Peng.** 2006. Homologous response regulators KvgA, KvhA, and KvhR regulate the synthesis of capsular polysaccharide in *Klebsiella pneumoniae* CG43 in a coordinated manner. J. Biochem. **140:**429–438.
26. **Lin, C. T., and H. L. Peng.** 2006. Regulation of the homologous two-component systems KvgAS and KvhAS in *Klebsiella pneumoniae* CG43. J. Biochem. **140:**639–648.
27. **Lin, J. C., F. Y. Chang, C. P. Fung, J. Z. Xu, H. P. Cheng, J. J. Wang, L. Y. Huang, and L. K. Siu.** 2004. High prevalence of phagocytic-resistant capsular serotypes of *Klebsiella pneumoniae* in liver abscess. Microbes Infect. **6:**1191–1198.
28. **Majdalani, N., and S. Gottesman.** 2005. The Rcs phosphorelay: a complex signal transduction system. Annu. Rev. Microbiol. **59:**379–405.
29. **Miller, J. H.** 1972. Experiments in molecular genetics. Cold Spring Harbor Laboratory Press, Cold Spring Harbor, NY.
30. **Mizuta, K., M. Ohta, M. Mori, T. Hasegawa, I. Nakashima, and N. Kato.** 1983. Virulence for mice of *Klebsiella* strains belonging to the O1 group: relationship to their capsular (K) types. Infect. Immun. **40:**56–61.
31. **Nassif, X., N. Honore, T. Vasselon, S. T. Cole, and P. J. Sansonetti.** 1989. Positive control of colanic acid synthesis in *Escherichia coli* by rmpA and rmpB, two virulence-plasmid genes of *Klebsiella pneumoniae*. Mol. Microbiol. **3:**1349–1359.
32. **Nassif, X., and P. J. Sansonetti.** 1986. Correlation of the virulence of *Klebsiella pneumoniae* K1 and K2 with the presence of a plasmid encoding aerobactin. Infect. Immun. **54:**603–608.
33. **Park, S. H., J. Eriksen, and S. D. Henriksen.** 1967. Structure of the capsular polysaccharide of *Klebsiella pneumoniae* type 2 (B). Acta Pathol. Microbiol. Scand. **69:**431–436.
34. **Peng, H. L., P. Y. Wang, J. L. Wu, C. T. Chiu, and H. Y. Chang.** 1991. Molecular epidemiology of *Klebsiella pneumoniae*. Zhonghua Min Guo Wei Sheng Wu Ji Mian Yi Xue Za Zhi **24:**264–271.
35. **Podschun, R., and U. Ullmann.** 1998. *Klebsiella* spp. as nosocomial pathogens: epidemiology, taxonomy, typing methods, and pathogenicity factors. Clin. Microbiol. Rev. **11:**589–603.
36. **Reed, L. J., and H. Muench.** 1938. A simple method of estimating fifty percent endpoints. Am. J. Hyg. **27:**493–497.
37. **Regueiro, V., M. A. Campos, J. Pons, S. Alberti, and J. A. Bengoechea.** 2006. The uptake of a *Klebsiella pneumoniae* capsule polysaccharide mutant triggers an inflammatory response by human airway epithelial cells. Microbiology **152:**555–566.
38. **Sambrook, J., E. F. Fritsch, and T. Maniatis.** 1989. Molecular cloning: a laboratory manual, 2nd ed. Cold Spring Harbor Laboratory, Cold Spring Harbor, NY.
39. **Schembri, M. A., J. Blom, K. A. Krogfelt, and P. Klemm.** 2005. Capsule and fimbria interaction in *Klebsiella pneumoniae*. Infect. Immun. **73:**4626–4633.
40. **Skorupski, K., and R. K. Taylor.** 1996. Positive selection vectors for allelic exchange. Gene **169:**47–52.
41. **Stout, V., A. Torres-Cabassa, M. R. Maurizi, D. Gutnick, and S. Gottesman.** 1991. RcsA, an unstable positive regulator of capsular polysaccharide synthesis. J. Bacteriol. **173:**1738–1747.
42. **Studier, F. W., A. H. Rosenberg, J. J. Dunn, and J. W. Dubendorff.** 1990. Use of T7 RNA polymerase to direct expression of cloned genes. Methods Enzymol. **185:**60–89.
43. **Vasil, M. L.** 2007. How we learnt about iron acquisition in *Pseudomonas aeruginosa*: a series of very fortunate events. Biometals **20:**587–601.
44. **Wacharotayankun, R., Y. Arakawa, M. Ohta, T. Hasegawa, M. Mori, T. Horii, and N. Kato.** 1992. Involvement of *rcsB* in *Klebsiella* K2 capsule synthesis in *Escherichia coli* K-12. J. Bacteriol. **174:**1063–1067.
45. **Wacharotayankun, R., Y. Arakawa, M. Ohta, K. Tanaka, T. Akashi, M. Mori, and N. Kato.** 1993. Enhancement of extracapsular polysaccharide synthesis in *Klebsiella pneumoniae* by RmpA2, which shows homology to NtrC and FixJ. Infect. Immun. **61:**3164–3174.
46. **Wang, F., S. Cheng, K. Sun, and L. Sun.** 2008. Molecular analysis of the *fur* (ferric uptake regulator) gene of a pathogenic *Edwardsiella tarda* strain. J. Microbiol. **46:**350–355.
47. **Wehland, M., and F. Bernhard.** 2000. The RcsAB box. Characterization of a new operator essential for the regulation of exopolysaccharide biosynthesis in enteric bacteria. J. Biol. Chem. **275:**7013–7020.
48. **Whitfield, C., and I. S. Roberts.** 1999. Structure, assembly and regulation of expression of capsules in *Escherichia coli*. Mol. Microbiol. **31:**1307–1319.
49. **Wu, K. M., L. H. Li, J. J. Yan, N. Tsao, T. L. Liao, H. C. Tsai, C. P. Fung, H. J. Chen, Y. M. Liu, J. T. Wang, C. T. Fang, S. C. Chang, H. Y. Shu, T. T. Liu, Y. T. Chen, Y. R. Shiau, T. L. Lauderdale, I. J. Su, R. Kirby, and S. F. Tsai.** 2009. Genome sequencing and comparative analysis of *Klebsiella pneumoniae* NTUH-K2044, a strain causing liver abscess and meningitis. J. Bacteriol. **191:**4492–4501.
50. **Wu, M. F., C. Y. Yang, T. L. Lin, J. T. Wang, F. L. Yang, S. H. Wu, B. S. Hu, T. Y. Chou, M. D. Tsai, C. H. Lin, and S. L. Hsieh.** 2009. Humoral immunity against capsule polysaccharide protects the host from *magA*$^+$ *Klebsiella pneumoniae*-induced lethal disease by evading Toll-like receptor 4 signaling. Infect. Immun. **77:**615–621.
51. **Yu, W. L., W. C. Ko, K. C. Cheng, H. C. Lee, D. S. Ke, C. C. Lee, C. P. Fung, and Y. C. Chuang.** 2006. Association between *rmpA* and *magA* genes and clinical syndromes caused by *Klebsiella pneumoniae* in Taiwan. Clin. Infect. Dis. **42:**1351–1358.